THE ASTROPHYSICAL JOURNAL, 546:248–266, 2001 January 1

PRESOLAR SiC GRAINS OF TYPE Y: ORIGIN FROM LOW-METALLICITY ASYMPTOTIC GIANT BRANCH STARS

SACHIKO AMARI,[1] LARRY R. NITTLER,[1,5] ERNST ZINNER,[1] ROBERTO GALLINO,[2] MARIA LUGARO,[3] AND ROY S. LEWIS[4]

Received 2000 February 16; accepted 2000 August 8

ABSTRACT

We report isotopic data for 27 presolar SiC grains of the rare subtype Y in an acid-resistant residue of the Murchison (CM2) meteorite. Presolar SiC grains of type Y constitute only ~1% of Murchison SiC grains larger than ~2 μm and are defined as having $^{12}C/^{13}C > 100$ (solar = 89) and $^{14}N/^{15}N > 272$ (solar). In a Si 3-isotope plot, their Si isotopic compositions plot to the right of the correlation line defined by the majority of presolar SiC grains (the mainstream population), whose isotopic compositions indicate an origin in C-rich asymptotic giant branch (AGB) stars of near-solar metallicity. Because of their low abundance, the new Y grains were identified by automatic isotopic imaging of the $^{12}C/^{13}C$ ratio in the ion microprobe. We report C, N, and Si isotopic ratios of all 27 grains, inferred initial $^{26}Al/^{27}Al$ ratios of 18, and Ti isotopic ratios of 20 grains. Whereas $^{14}N/^{15}N$ and $^{26}Al/^{27}Al$ ratios exhibit the same range as mainstream grains, the C, Si, and Ti isotopic ratios are distinct. Carbon-12/carbon-13 ratios range up to 295 and $^{30}Si/^{28}Si$ excesses up to 183‰ relative to solar. The average $^{29}Si/^{28}Si$ ratio of Y grains is by 59‰ smaller than that of mainstream grains. Ti isotopic ratios relative to ^{48}Ti are somewhat similar to those of mainstream grains, but extend to more extreme anomalous compositions. One grain has $^{46}Ti/^{48}Ti$, $^{49}Ti/^{48}Ti$, and $^{50}Ti/^{48}Ti$ excesses of 183‰, 365‰, and 990‰, respectively, relative to solar. These features exhibited by Y grains point to an origin in AGB stars of somewhat lower than solar metallicity. In the envelope of such stars the proportion of ^{12}C and *s*-processed material dredged up from deep zones that experienced partial He burning and was mixed with original material is higher than in stars of solar metallicity. Their envelopes are therefore expected to have larger $^{12}C/^{13}C$, $^{30}Si/^{28}Si$, and $^{49}Ti/^{48}Ti$ and $^{50}Ti/^{48}Ti$ ratios than mainstream grains. We compare the C, Si, and Ti isotopic compositions of Y grains with the results of theoretical models of AGB stars with 1.5, 3, and 5 $M_\odot$ and $Z = 0.006$, 0.01, and 0.02. While solar-metallicity ($Z = 0.02$) AGB models cannot account for the Y grain data, the models with $Z = 0.01$ can reproduce the measured isotopic compositions reasonably well. A range of stellar masses (from 1.5 $M_\odot$ possibly up to 5 $M_\odot$) is indicated by the grain data. The present study together with additional data on SiC grains of type Z furthermore indicate that the rate of change of the ratios of the secondary Si isotopes (^{29}Si and ^{30}Si) relative to ^{28}Si prior to solar system formation was lower than has been generally assumed, implying larger contributions of ^{28}Si from Type Ia supernovae compared to those from Type II supernovae. The Si isotopic ratios of Galactic cosmic rays also suggest such an evolution.

Subject headings: dust, extinction — Galaxy: evolution — ISM: abundances — nuclear reactions, nucleosynthesis, abundances — stars: AGB and post-AGB

On-line material: color figures

1. INTRODUCTION

More than 10 years have passed since Lewis et al. (1987) isolated and identified presolar diamond from the Allende meteorite, opening a new field of astronomy: the study of presolar grains in meteorites. Presolar grains are mineral dust grains that formed in the circumstellar envelopes of late-type stars and in supernova (SN) ejecta before the solar system was born, survived destruction in the interstellar medium (ISM), and were trapped as pristine relics in primitive meteorites. Other types of presolar grains, including silicon carbide (Bernatowicz et al. 1987; Tang & Anders 1988), graphite (Amari et al. 1990), corundum (Nittler et al. 1994; Hutcheon et al. 1994; Huss et al. 1994), hibonite (Choi, Wasserburg, & Huss 1999), silicon nitride (Nittler et al. 1995), and refractory carbides (Bernatowicz et al. 1991, 1996) have been discovered in meteorites in subsequent years. The great majority of presolar grains found to date have been identified in acid-resistant separates of chondritic meteorites.

Proof of the stellar origin of presolar grains comes from huge isotopic deviations from the solar system ratios, which can only be achieved by nucleosynthesis taking place in stars. Thus, a small portion of the protosolar-nebula material must have survived intact the formation of the solar system and subsequent parent body processes and was retained in primitive meteorites.

Among the types of presolar grains identified to date, SiC has been widely studied because it is present in various types of meteorites, it is the second most abundant type after diamond (Huss & Lewis 1995), and because its trace

[1] Laboratory for the Space Sciences and the Physics Department, Washington University, One Brookings Drive, St. Louis, MO 63130; sa@howdy.wustl.edu, ekz@howdy.wustl.edu.

[2] Dipartimento di Fisica Generale, Università di Torino, Via P. Giuria 1, I-10125 Torino, Italy; gallino@ph02xd.ph.unito.it.

[3] Department of Mathematics, Monash University, Clayton 3168, Victoria, Australia; marial@thala.maths.monash.edu.au.

[4] Enrico Fermi Institute, University of Chicago, 5630 Ellis Avenue, Chicago, IL 60637; royl@rainbow.uchicago.edu.

[5] Present address: Laboratory for Extraterrestrial Physics, Code 691, NASA Goddard Spaceflight Center, Greenbelt, MD 20771; nittler@lepvax.gsfc.nasa.gov.

element abundances are relatively high (Amari et al. 1995), allowing isotopic ratios of multiple elements to be determined in single grains. Isotopic ratios of noble gases (Lewis, Amari, & Anders 1990, 1994), Sr (Ott & Begemann 1990a; Prombo et al. 1992), Ba (Ott & Begemann 1990b; Zinner, Amari, & Lewis 1991; Prombo et al. 1993), Nd (Zinner et al. 1991; Richter, Ott, & Begemann 1993), and Sm (Zinner et al. 1991; Richter et al. 1993) have been measured on aggregates of grains (≡bulk samples). These data show strong signatures of the slow neutron capture process (*s* process), indicating that a majority of the SiC grains had formed in C-rich asymptotic giant branch (AGB) stars, which are believed to be the major source of the heavy *s*-process elements from the Sr-Y-Zr peak to Pb in the universe. Gallino et al. (1990, 1993, 1997) could successfully reproduce the heavy-element isotopic patterns by model calculations of AGB stars experiencing thermal pulses (TP), and they concluded that the majority of presolar SiC grains most likely formed in low-mass (1.5–3 $M_{\odot}$) AGB stars of solar metallicity. Grain formation must have taken place in the late stages of AGB evolution, when repeated third dredge-up (TDU) of ^{12}C from the He shell turned the star into a carbon star with C > O, a necessary condition for the condensation of SiC.

Analysis of individual SiC grains by ion microprobe mass spectrometry revealed the presence of several distinct populations, which are distinguished by the isotopic compositions of mainly C and Si. The majority of grains (about 94%) are known as the mainstream population. The rest is comprised of the minor populations A, B, X, Y, and Z (see, e.g., Hoppe & Ott 1997). Mainstream grains have $^{12}C/^{13}C$ ratios between 10 and 100 (Fig. 1). The distribution of this ratio is very similar to that observed in carbon stars (see Fig. 3 of Hoppe & Ott 1997) and agrees with model calculations of AGB stars of 1.5–3 $M_{\odot}$ with solar metallicity. Nitrogen is isotopically light and $^{26}Al/^{27}Al$ ratios, inferred from excesses of radiogenic ^{26}Mg, range from 10^{-5} up to 10^{-3}. Silicon is enriched in ^{29}Si and ^{30}Si. In the 3-isotope plot of $\delta^{29}Si/^{28}Si$ versus $\delta^{30}Si/^{28}Si$ {δ-values are deviations from the solar ratios in permil, i.e., $\delta^{i}Si/^{28}Si \equiv [(^{i}Si/^{28}Si)_{meas}/(^{i}Si/^{28}Si)_{solar} - 1] \times 1000$}, the data cluster along a line of slope 1.31 (see Lugaro et al. 1999 and Fig. 2).

Grains of type A and B (~3%–4%) have $^{12}C/^{13}C < 10$ (Hoppe et al. 1994, 1996a; Amari et al. 1997b, 2000a). Many grains have isotopically heavy N and higher $^{26}Al/^{27}Al$ ratios than mainstream grains. However, Si isotopic ratios are in the same range as those of mainstream grains ($^{29}Si/^{28}Si$ and $^{30}Si/^{28}Si$ excesses of up to 150‰ compared to solar), making it impossible to distinguish them from mainstream grains in a Si 3-isotope plot. Carbon stars of type J (Hoppe et al. 1994) and CH stars (Lodders & Fegley 1995, 1998) have been proposed as their stellar sources.

SiC grains of type X (~1%) are characterized by ^{28}Si excesses up to 5 times compared to the solar Si isotopic ratios (Amari et al. 1992; Nittler et al. 1995). They have mostly light C and large ^{15}N excesses and exhibit the largest inferred $^{26}Al/^{27}Al$ ratios (up to 0.6). The inferred presence of extinct radioactive ^{44}Ti ($T_{1/2} = 60$ yr) in some of these grains is proof of their SN origin (Hoppe et al. 1996c; Nittler et al. 1996). The isotopic signatures of X grains are similar to those of low-density round graphite grains, which are also believed to have a SN origin (Travaglio et al. 1999).

Grains of type Z have subsolar $^{29}Si/^{28}Si$ ratios and large $\delta^{30}Si/^{28}Si$ values compared to their $\delta^{29}Si/^{28}Si$ values

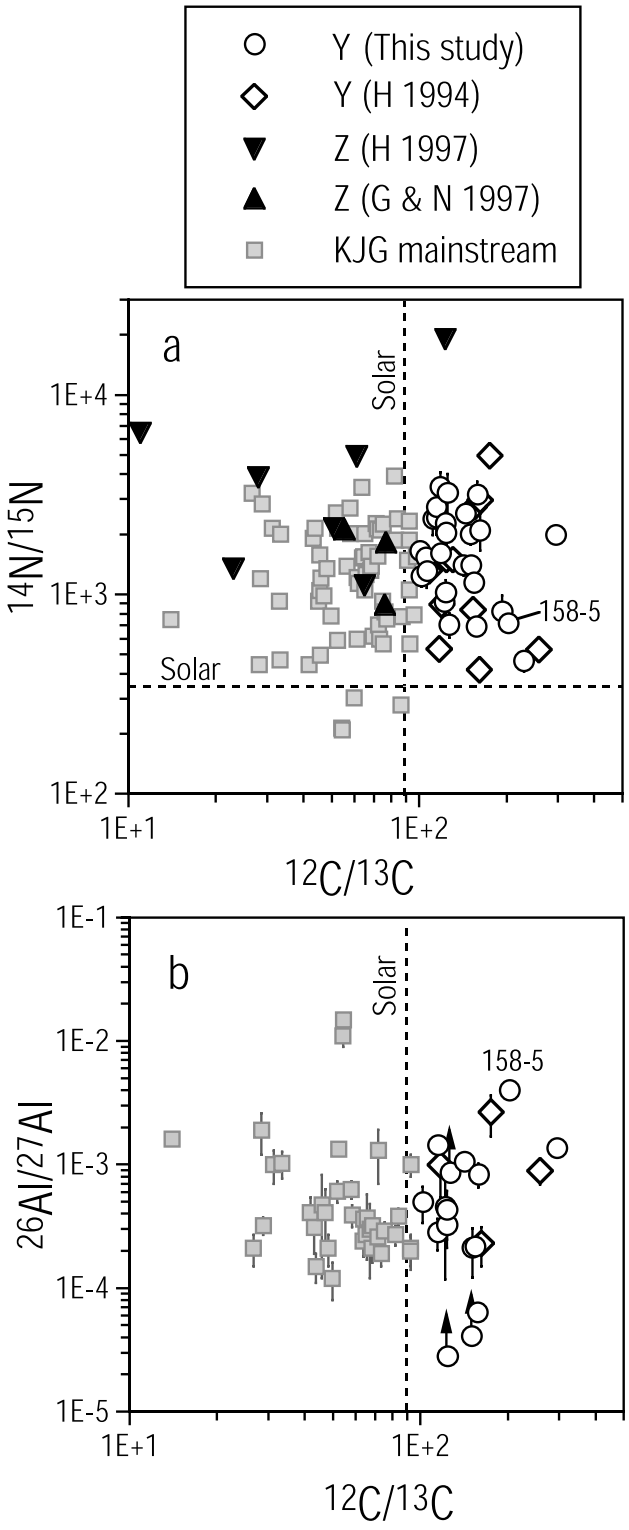

FIG. 1.—Nitrogen, carbon, and aluminum isotopic ratios of SiC grains of type Y from this study and the study by Hoppe et al. (1994). Also plotted are the ratios measured in mainstream grains (Hoppe et al. 1994) and in Z grains (Hoppe et al. 1997; Gao & Nittler 1997). Y grains are defined as grains with $^{12}C/^{13}C > 100$ and $^{14}N/^{15}N >$ solar. The broken lines indicate the solar N and C isotopic ratios. Grain 158-5 (short for KJGM1-158-5) is the grain with the most extreme Al, Si, and Ti isotopic ratios (Table 1). Error bars in this and subsequent figures are 1 σ. See the electronic edition of the Journal for a color version of this figure.

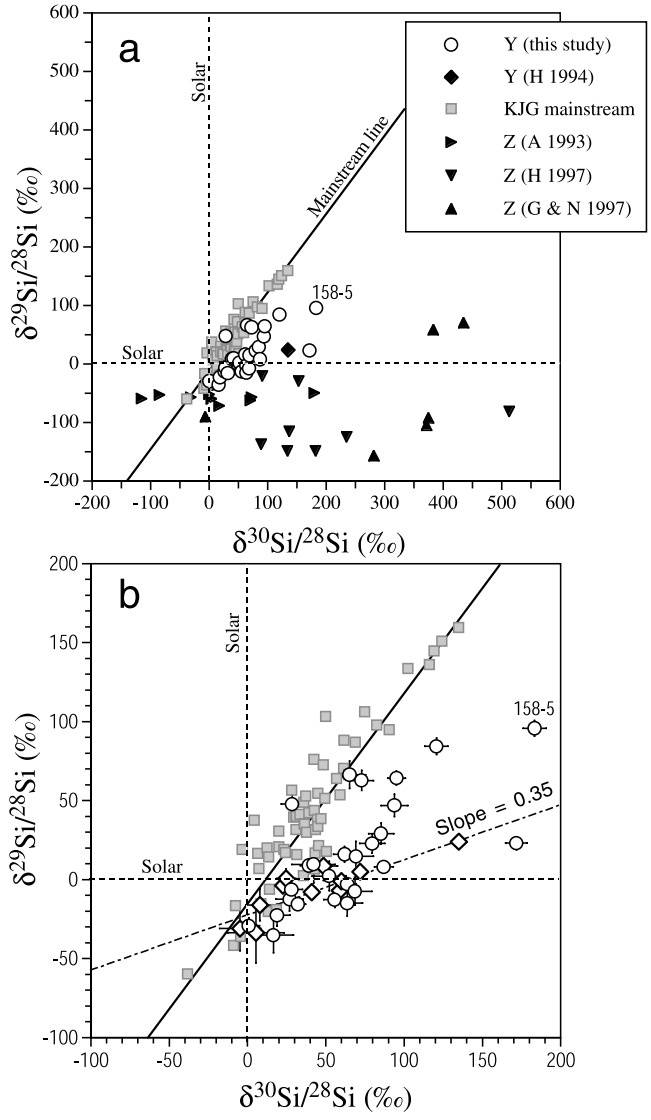

FIG. 2.—Silicon isotopic ratios of Y grains. The ratios are plotted as δ-values, deviations in permil from the solar system ratios. Also plotted are the ratios of several Z grains (Alexander 1993; Hoppe et al. 1997; Gao & Nittler 1997) and of the KJG mainstream grains (Hoppe et al. 1994). The mainstream line is the best-fit line to mainstream grains from the Murchison and Orgueil meteorites (see Lugaro et al. 1999). The slope = 0.35 line in the lower graph is the best-fit line to the ratios of six Y grains identified by Hoppe et al. (1994). See the electronic edition of the Journal for a color version of this figure.

(Alexander 1993). Among grains greater than 2 μm they are even rarer than X grains but their abundance appears to increase with decreasing grains size (Hoppe et al. 1999). Most have C and N isotopic ratios within the range of mainstream grains. Hoppe et al. (1997) proposed that they formed in low-metallicity ($\sim 1/3\ Z_{\odot}$), low-mass ($< 2.3\ M_{\odot}$) AGB stars. Some, however, have very low $^{12}C/^{13}C$ and $^{14}N/^{15}N$ ratios and probably come from novae (Gao & Nittler 1997).

More detailed descriptions of these types of grains can be found in the review papers by Hoppe & Ott (1997) and Zinner (1998), and references cited therein.

Grains of type Y were originally identified in the Murchison KJG and KJH SiC separates as a distinct population ($\sim 1\%$) with $^{12}C/^{13}C$ ratios higher than 140 but N and Si isotopic ratios distinct from those of X grains (Hoppe et al. 1994). Subsequent studies have lowered the $^{12}C/^{13}C$ ratio that distinguishes Y grains from mainstream ones to 100 (Hoppe & Ott 1997; Zinner 1998) and we use this definition here. Almost all Y grains have ^{30}Si excesses relative to mainstream grains, so that in a Si 3-isotope plot they lie to the right of the mainstream correlation line. Since their N and inferred Al ratios are similar to those of mainstream grains, an AGB star origin has been proposed for Y grains (Hoppe et al. 1994; Amari et al. 1997a). The six Y grains originally identified by Hoppe et al. (1994) lie on a slope 0.35 line in a Si 3-isotope plot and were considered to have originated from a single AGB star. This slope was believed to be consistent with the value predicted for the evolution of the envelope composition of a solar-metallicity AGB star during repeated TDU episodes in the TP phase (however, see Lugaro et al. 1999 for a more recent evaluation).

Because of the low abundance of Y grains, only a few have been analyzed in detail in the past (Hoppe et al. 1994). In this paper, we present the isotopic compositions of 27 new Y grains identified by an automatic high–mass-resolution ion-imaging technique and subsequently analyzed for their isotopic compositions using conventional ion microprobe techniques. We compare the observed isotopic ratios with those of mainstream grains in the same size range and with model calculations of nucleosynthesis and mixing in AGB stars to obtain a better insight into their origin. For this comparison we added the Y grains studied by Hoppe et al. (1994) to our data set. It should be mentioned that Y grains have been identified in other previous studies. Alexander (1993) found several in the study of SiC from a variety of ordinary chondrites, Hoppe et al. (1996b) in the study of smaller grain size fractions from the Murchison KJ series, and Huss, Hutcheon, & Wasserburg (1997) in the study of SiC grains from the C1 meteorite Orgueil. However, Alexander (1993) did not measure N isotopic ratios and the size of the grains is not known; the Y grains of the Hoppe et al. (1996b) study are much smaller than those of the present study and errors on the Si isotopic ratios are much larger; furthermore, none of the grains of these three studies had their Ti isotopic ratios measured. For these reasons we do not include them in the present discussion.

2. EXPERIMENTAL PROCEDURES

2.1. *Sample Preparation*

A detailed description of the presolar grain separation technique is given by Amari, Lewis, & Anders (1994). Thus, only a brief summary is given here.

Approximately 83 g of the Murchison meteorite (Me 2752, Field Museum of National History) was treated alternately by HCl-HF and HCl to dissolve silicates and insoluble fluoride, which forms protective coatings and prevents the further dissolution of silicates. After this treatment, sulfur and reactive kerogen were removed with 4M KOH and H_2O_2. Presolar diamond was extracted by colloidal separation with 0.1M NH_3. Subsequently, the sample was treated with 0.5N $Na_2Cr_2O_7$–$2NH_2SO_4$ to further remove any reactive kerogen.

By density separation, presolar graphite was extracted from fractions with density 1.6–2.2 g cm^{-3}. A fraction with density greater than 2.3 g cm^{-3} was treated with $HClO_4$ to remove any remaining carbon and chromite, and then with

H_2SO_4 to destroy spinel. The remaining residue consisted mainly of SiC. Size separation yielded nine fractions (KJA-KJI). The third coarsest fraction, KJG, with an average grain diameter of 3.02 μm, was used for this study.

2.2. *High–Mass-Resolution Ion Imaging*

Because of the low abundance of Y grains, it is necessary to use an automatic search procedure to obtain a sufficient number of grains for analysis. A few Y grains have previously been discovered in fractions KJG and KJH (average grain diameter 4.57 μm) and are added to this study. Additional Y grains found in smaller Murchison fractions and in other meteorites (Alexander 1993; Hoppe et al. 1996b; Huss et al. 1997) will not be discussed here. Ion imaging techniques have been previously developed to rapidly determine isotopic ratios in large numbers of grains in order to identify rare types of grains with distinct isotopic compositions. For example, ion imaging has been used to identify both presolar oxide grains (Nittler et al. 1994, 1997) and SiC grains of type X (Nittler et al. 1995; Hoppe et al. 1996c). The method is described in detail by Nittler (Nittler 1996; Nittler et al. 1995, 1997) and Hoppe et al. (1996c).

SiC grains of type Y are defined by their high $^{12}C/^{13}C$ ratios (>100). Whereas the search for presolar oxide grains and for SiC grains of type X can be accomplished by low–mass-resolution ion imaging measurement of the $^{18}O/^{16}O$ and $^{30}Si/^{28}Si$ ratios, respectively, the automatic search for Y grains requires high–mass-resolution conditions in order to separate the ^{12}CH interference from ^{13}C. Imaging searches for Y grains were made at a mass resolving power ($m/\Delta m$) of $\sim$3000, sufficient for the C isotopic measurement. Direct ion images ($\sim$70 μm by 70 μm) of ^{12}C and ^{13}C were produced by the Washington University ion microprobe and digitized by a slow-scan CCD camera. Individual SiC grains were identified in the ion images and $^{12}C/^{13}C$ ratios determined by image processing techniques. Ion imaging of a synthetic SiC standard indicates a 2 σ precision of $\sim$2% in the measurement of $^{12}C/^{13}C$, sufficient to distinguish Y grains from mainstream grains.

Two mounts (KJGM1 and KJGM4C) were analyzed by high–mass-resolution ion imaging; about 1400 SiC grains were measured on each. A total of 138 Y grain candidates were identified on the basis of having $^{12}C/^{13}C$ ratios greater than 100. Subsequent C and N isotopic measurements by conventional (i.e., not ion imaging) ion probe techniques (Zinner, Tang, & Anders 1989) of the candidates confirmed 27 as Y grains. Fifteen additional candidates were identified as X grains on the basis of their Si isotopic compositions, and the remaining candidates were mainstream grains. The apparent high $^{12}C/^{13}C$ ratios determined by ion imaging in the latter grains were probably the result of statistical fluctuations, given the relatively large error of the ion imaging measurement. We further analyzed the Y grains for their isotopic compositions of Mg-Al (18 grains), Si (26 grains), and Ti (20 grains), using conventional high–mass-resolution ion probe techniques.

3. RESULTS

In this section, we will present the results obtained for Y grains together with previously obtained data of mainstream (Hoppe et al. 1994) and Z grains (Gao & Nittler 1997; Hoppe et al. 1997). This is because, as discussed in the following sections, these three populations, judging from their isotopic ratios (although different in their average $\delta^{29}Si/^{28}Si$ values) seem to have a common origin, in C-rich AGB stars (Lewis et al. 1990, 1994; Hoppe et al. 1994; Hoppe & Ott 1997; Huss et al. 1997). Table 1 contains the isotopic data of this study and of the Y grains studied by Hoppe et al. (1994).

3.1. C *and* N *Isotopic Ratios*

Carbon and N isotopic ratios of the Y grains of this study are plotted in Figure 1*a*. Also plotted in the figure are KJG mainstream grains, previously measured Y grains, and Z grains. Although the size distribution of these Z grains has not been determined, they are, on average, much smaller than the Y and mainstream grains plotted here and in subsequent figures. The $^{12}C/^{13}C$ ratios of Y grains range from 100 up to 300. Z grains have a C isotopic range similar to that of mainstream grains. The distribution of N isotopic ratios of Y grains is similar to that of mainstream grains. A few of the Z grains measured by Hoppe et al. (1997) have higher $^{14}N/^{15}N$ ratios than the Y grains. This may not be an intrinsic property of Z grains, but rather a grain-size effect. Hoppe et al. (1996b) have found that smaller SiC grains tend to have higher $^{14}N/^{15}N$ ratios and the Z grains identified by Hoppe et al. (1997) are from the KJE fraction (mean size $\sim$1 μm) and are hence smaller than the KJG grains reported here ($\sim$3 μm).

3.2. *Aluminum-26/Aluminum-27 Ratios*

Inferred $^{26}Al/^{27}Al$ ratios of the 18 Y grains analyzed for Mg-Al are shown in Figure 1*b*. For three grains, due to the proximity of Al-rich oxide grains on the sample mount, only lower limits were obtained. $^{26}Al/^{27}Al$ ratios range from 6×10^{-5} to 4×10^{-3}. This range is similar to that observed in mainstream grains. Hoppe et al. (1997) reported a value of 2×10^{-3} for $^{26}Al/^{27}Al$ in one Z grain; this value is again similar to typical values observed in mainstream SiC grains.

3.3. Si *Isotopic Ratios*

Silicon isotopic ratios of mainstream grains show a linear correlation (Figs. 2*a* and 2*b*). Only mainstream grains from separate KJG are plotted in the figure but the same correlation is shown by mainstream grains of other size fractions of SiC from Murchison (Hoppe et al. 1994, 1996b) and from other meteorites (Alexander 1993; Huss et al. 1997). The regression line has a slope of 1.31 and intercepts the $\delta^{29}Si/^{28}Si$ axis at $-15.9‰$. Most mainstream grains show excesses in the neutron-rich Si isotopes. Almost all Y grains plot to the right of the regression line, indicating that they are enriched in ^{30}Si (or depleted in ^{29}Si) relative to mainstream SiC. On average, Y grains have smaller $\delta^{29}Si/^{28}Si$ values than mainstream grains. The mean and the standard deviation of $\delta^{29}Si/^{28}Si$ are 4.6‰ and 33.2‰, respectively, the former being significantly smaller than the mean of mainstream SiC (50.4‰ with a standard deviation of 42.7‰). Grains KJGM1-158-5 ($\delta^{30}Si/^{28}Si = 183 \pm 7‰$) and KJGM1-337-3 ($\delta^{30}Si/^{28}Si = 172 \pm 7‰$) have the largest $\delta^{30}Si/^{28}Si$ values; their horizontal distances from the mainstream correlation line are 98 ± 8 and 142 ± 7, respectively. Most Z grains lie also on the right side of the mainstream line. Silicon-30 in many Z grains is even more enriched than in Y grains, with $\delta^{30}Si/^{28}Si$ values ranging from $-116‰$ to 1118‰ and showing much more scatter than do the other two types of grains. Their mean $\delta^{29}Si/^{28}Si$ value ($-68.8‰$ with a standard deviation of 66.8‰) is the lowest among the three populations of grains.

TABLE 1

ISOTOPIC RATIOS OF Y GRAINS

Grain	$^{12}C/^{13}C$	$^{14}N/^{15}N$	$^{26}Al/^{27}Al$ ($\times 10^{-4}$)	$\delta^{29}Si/^{28}Si$ (‰)	$\delta^{30}Si/^{28}Si$ (‰)	$\delta^{46}Ti/^{48}Ti$ (‰)	$\delta^{47}Ti/^{48}Ti$ (‰)	$\delta^{49}Ti/^{48}Ti$ (‰)	$\delta^{50}Ti/^{48}Ti$ (‰)
KJGM1-158-5	203 ± 3	718 ± 75	40.0 ± 2.2	95.8 ± 4.9	183.4 ± 7.3	238 ± 32	23 ± 28	365 ± 40	990 ± 55
KJGM1-189-1	123 ± 2	2275 ± 410	3.26 ± 1.14	22.9 ± 6.1	79.6 ± 8.1	−15 ± 43	−25 ± 44	−80 ± 51	−12 ± 79
KJGM1-231-8	145 ± 3	2544 ± 257	<1.23	−12.7 ± 4.8	55.6 ± 6.9	−40 ± 27	−20 ± 28	−17 ± 33	63 ± 36
KJGM1-293-7	125 ± 4	3240 ± 766	<0.16	10 ± 12	42 ± 14	…	…	…	…
KJGM1-295-2	151 ± 4	1401 ± 144	2.13 ± 0.92	−7.4 ± 8.5	69 ± 11	−93 ± 61	−44 ± 65	−9 ± 79	354 ± 99
KJGM1-337-3	295 ± 6	1994 ± 159	13.6 ± 0.8	23.0 ± 4.2	171.7 ± 6.8	…	…	…	…
KJGM1-343-4	119 ± 2	1610 ± 183	…	−29.2 ± 5.0	0.9 ± 6.8	18 ± 37	2 ± 37	89 ± 46	156 ± 49
KJGM1-363-1	142 ± 3	1402 ± 158	10.6 ± 0.8	84.3 ± 5.2	120.6 ± 7.3	75 ± 36	74 ± 36	80 ± 43	274 ± 49
KJGM1-444-1	115 ± 3	2424 ± 423	2.84 ± 0.81	66.3 ± 8.6	65 ± 10	30 ± 40	15 ± 40	140 ± 51	217 ± 55
KJGM1-77-2	154 ± 3	1146 ± 68	2.17 ± 0.09	16.0 ± 5.0	62.0 ± 7.0	114 ± 30	46 ± 29	251 ± 38	170 ± 41
KJGM1-84-3	157 ± 2	691 ± 40	0.639 ± 0.041	8.0 ± 4.0	87.0 ± 6.0	…	…	…	…
KJGM4C-110-2	229 ± 7	465 ± 53	…	62.8 ± 6.3	72.8 ± 7.5	21 ± 62	−8 ± 63	194 ± 84	54 ± 79
KJGM4C-161-1	123 ± 2	1024 ± 158	4.30 ± 1.83	−15.6 ± 3.7	32.2 ± 4.9	…	…	…	…
KJGM4C192-2	127 ± 2	706 ± 99	>8.63	47.8 ± 5.8	28.5 ± 6.8	20 ± 44	−11 ± 45	78 ± 56	98 ± 58
KJGM4C-261-2	112 ± 3	2388 ± 405	…	−12.5 ± 7.4	26.9 ± 8.8	−63 ± 75	−53 ± 78	−107 ± 89	−10 ± 97
KJGM4C-271-2	102 ± 2	1238 ± 144	4.98 ± 1.60	8.9 ± 4.3	39.2 ± 5.5	91 ± 23	24 ± 23	91 ± 28	273 ± 32
KJGM4C-305-2	101 ± 2	1650 ± 151	…	…	…	…	…	…	…
KJGM4C-344-2	124 ± 3	2039 ± 264	>0.28	−6.3 ± 5.7	28.0 ± 6.9	…	…	…	…
KJGM4C-347-2	150 ± 5	2000 ± 217	>0.41	−22.6 ± 6.9	18.8 ± 8.2	33 ± 46	1 ± 47	169 ± 61	60 ± 56
KJGM4C-4-2	122 ± 3	920 ± 171	4.56 ± 3.39	14.6 ± 9.5	69 ± 11	180 ± 64	152 ± 65	135 ± 75	407 ± 91
KJGM4C-40-2	159 ± 4	3163 ± 515	8.34 ± 1.81	−14.9 ± 8.1	63.7 ± 9.7	…	…	…	…
KJGM4C-43-3	106 ± 2	1309 ± 232	…	2.3 ± 9.2	52 ± 11	173 ± 58	65 ± 55	196 ± 71	376 ± 79
KJGM4C-43-4	106 ± 2	1537 ± 199	…	46.9 ± 7.1	93.8 ± 8.5	90 ± 33	−62 ± 30	47 ± 39	143 ± 42
KJGM4C-60-6	118 ± 3	3468 ± 622	…	−35 ± 11	17 ± 13	53 ± 58	20 ± 58	45 ± 70	74 ± 73
KJGM4C-61-1	162 ± 3	2093 ± 436	…	−2.8 ± 4.1	63.7 ± 5.4	−7 ± 19	−7 ± 20	−8 ± 23	154 ± 26
KJGM4C-70-4	115 ± 2	2747 ± 372	14.4 ± 1.29	64.2 ± 4.3	95.2 ± 5.6	32 ± 35	88 ± 37	44 ± 43	96 ± 45
KJGM4C-80-3	193 ± 5	824 ± 163	…	29.1 ± 6.6	85.3 ± 8.0	−3 ± 44	−65 ± 43	117 ± 58	457 ± 70
KJH3-042 (Y1)[a]	175 ± 1	4954 ± 1801	26.5 ± 9.7	5 ± 3	72 ± 3	…	…	…	…
KJH3-202 (Y2)[a]	162 ± 2	2962 ± 644	2.27 ± 0.75	−8 ± 1	41 ± 1	…	…	…	…
KJG4-0402 (Y3)[a]	153 ± 6	838 ± 36	…	−7 ± 5	59 ± 3	−27 ± 28	−25 ± 31	15 ± 27	125 ± 34
KJH5-851 (Y4)[a]	258 ± 9	529 ± 60	8.9 ± 0.2	24 ± 3	135 ± 3	…	…	…	…
KJH5-7m14 (Y5)[a]	161 ± 4	419 ± 31	…	−1 ± 4	60 ± 4	2 ± 11	−2 ± 13	−36 ± 12	65 ± 10
KJG2-157 (Y6)[a]	155 ± 2	2751 ± 222	…	−16 ± 10	8 ± 9	…	…	…	…
KJG2-067.1[a]	120 ± 1	890 ± 139	…	9 ± 9	48 ± 9	…	…	…	…
KJG2-142.1[a]	124 ± 2	1492 ± 177	…	−31 ± 14	−5 ± 13	…	…	…	…
KJG2-233.1[a]	130 ± 3	1493 ± 458	…	−34 ± 19	5 ± 18	…	…	…	…
KJH9-041.1[a]	108 ± 2	1313 ± 126	…	−4 ± 5	23 ± 5	…	…	…	…
KJH7-561.1[a]	117 ± 3	534 ± 42	9.9 ± 4.6	1 ± 6	25 ± 6	…	…	…	…

[a] Data from Hoppe et al. 1994.

3.4. Ti *Isotopic Ratios*

Ti-isotopic ratios are plotted in Figure 3. Along with the Y grain data we also plotted measurements on mainstream grains from KJH (Hoppe et al. 1994) and from a Murchison SiC separate (MUR) > 1.5 μm in diameter (Alexander & Nittler 1999). It should be noted that the KJH mainstream grains whose Ti isotopes have been measured were not selected at random but grains with large ^{29}Si and ^{30}Si excesses were preferentially chosen for analysis. On the other hand, Alexander & Nittler (1999) chose for their analysis grains with high Ti concentrations. The analyzed mainstream grains thus do not form a representative sample. The Ti isotopic ratios of the Y grains span a somewhat larger range than the mainstream grains from MUR and even from KJH. Grain KJGM1-158-5 is especially unusual; it exceeds all the others in its $\delta^{46}Ti/^{48}Ti$, $\delta^{49}Ti/^{48}Ti$, and $\delta^{50}Ti/^{48}Ti$ values. As pointed out in the previous section, this grain also has the largest ^{30}Si excess observed among the Y grains (see Table 1 and Fig. 2).

The Ti-isotopic patterns of the 16 Y grains that have deviations from solar by more than 2 σ in at least one isotopic ratio are shown in Figure 4. Four other grains are isotopically normal within rather large error bars and of another seven grains of this study not enough material was left for Ti isotopic analysis. Seven of the grains plotted in Figure 4 exhibit enrichments in both light and heavy isotopes relative to ^{48}Ti. That type of pattern is also observed in mainstream SiC (Hoppe et al. 1994), as well as in X grains (Nittler et al. 1996) and in low-density graphite grains of SN origin (Travaglio et al. 1999). The other grains show enrichment only in the heavy isotopes. Significant excesses in only ^{50}Ti are observed in half of the grains, $\delta^{46}Ti/^{48}Ti$ and $\delta^{47}Ti/^{48}Ti$ values being near normal. It should be noted that enrichments of only the heavy Ti isotopes have been also observed in A and B grains (Amari et al. 1999).

3.5. *Trace Element Abundances*

In this study we were unable to measure trace element abundances of any of Y grains, since most grains were consumed during Ti-isotopic analysis. However, trace element data on Y grains are available. Amari et al. (1995) measured elemental abundances of two Y grains from KJH (Fig. 5).

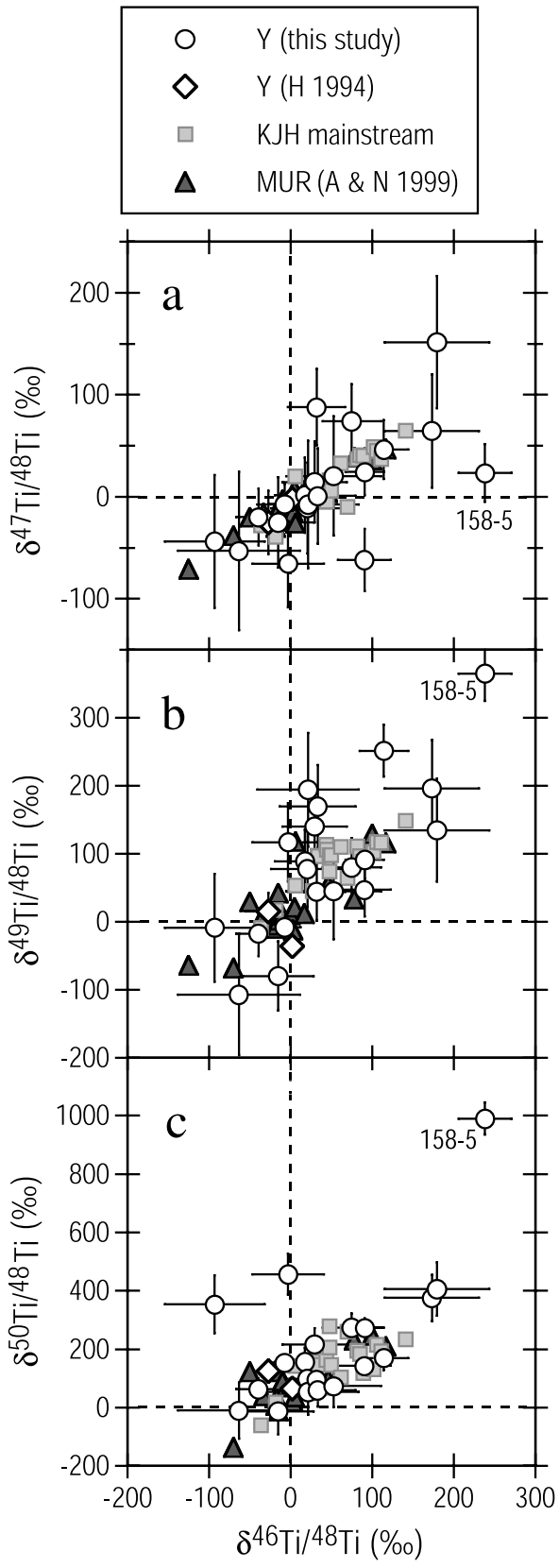

FIG. 3.—Titanium isotopic ratios of Y grains. Also plotted are the ratios measured in KJH mainstream grains (Hoppe et al. 1994) and in Murchison SiC grains (Alexander & Nittler 1999). To avoid clutter, no error bars are plotted for the mainstream grains. See the electronic edition of the Journal for a color version of this figure.

Abundances are normalized to Si and the solar system (Anders & Grevesse 1989). Thus, elements of solar abundance relative to Si lie on the dotted line. The two Y grains have a remarkably similar pattern. They are enriched in Ti and V as well as the heavy *s*-process elements Y, Zr, Ba, and Ce relative to the average of mainstream grains. Lodders & Fegley (1995) calculated the condensation of solids from a carbon-rich (C > O) gas of otherwise solar composition, simulating the condensation of minerals from the envelope of AGB stars. They showed that about 55% of the Si would condense into SiC. According to this result, the overabundance of Ti and V in the two Y grains is explained if both elements completely condensed into SiC either as solid solution or as carbide grains inside of SiC. Smaller grain size fractions from the KJ series also show this overabundance of Ti and V (Amari et al. 1995) and only the average of the large KJH grains has low concentration. Note that the abundance ratio of the heavy elements (Sr-Ce) relative to Ti and V is the same in the two Y grains as in the mainstream grains. It remains to be seen whether this is typical for all Y grains.

4. DISCUSSION

4.1. *Mainstream* SiC *Grains and AGB Stars*

Mainstream SiC grains are, as mentioned above, widely believed to have formed in the envelopes of C-rich AGB stars. The evolution of stars to the AGB phase (Iben & Renzini 1982; Lattanzio & Boothroyd 1997; Straniero et al. 1997; Gallino et al. 1998; Lattanzio & Forestini 1999; Blöcker 1999), the nucleosynthesis in AGB stars (Gallino et al. 1997, 1998; Busso, Gallino, & Wasserburg 1999) and the isotopic composition of mainstream SiC grains (Hoppe et al. 1994; Hoppe & Ott 1997; Timmes & Clayton 1996; Huss et al. 1997; Zinner 1998; Alexander & Nittler 1999; Lugaro et al. 1999) have been previously discussed in detail and shall not be repeated. We give here a short synopsis of the most important features.

AGB stars are low-to-intermediate mass ($M \lesssim 8\ M_{\odot}$) stars in the late stages of their evolution. They consist of a C and O degenerate core and thin He and H shells surrounding the core, which burn alternately during the TP-AGB phase. The extended envelope experiences considerable mass loss by stellar winds, eventually leaving behind the C-O core as a white dwarf progenitor. During thermal pulses, partial burning of He produces ^{12}C in the He-shell. The He-burning shell becomes convective, spreading over the whole He intershell, that is the thin region between the H and the He shells. Furthermore, *s*-process nucleosynthesis occurs in a tiny layer (the "^{13}C pocket") on top of the He intershell, where the ^{13}C(α, n)^{16}O reaction produces neutrons under radiative conditions during the interpulse periods, and, to a minor extent, in the convective TP where the ^{22}Ne neutron source is activated (Straniero et al. 1997; Gallino et al. 1998).

After a few thermal pulses the convective envelope penetrates into the He intershell at the quenching of each thermal instability (third dredge-up episodes, TDU). This means that in the TP-AGB phase material in the He and H shell is repeatedly dredged up and mixed with material in the envelope. As the envelope becomes enriched in material from the He shell, in particular newly synthesized ^{12}C and *s*-process elements, its C content increases until C/O > 1 and the star becomes a carbon star. This condition is

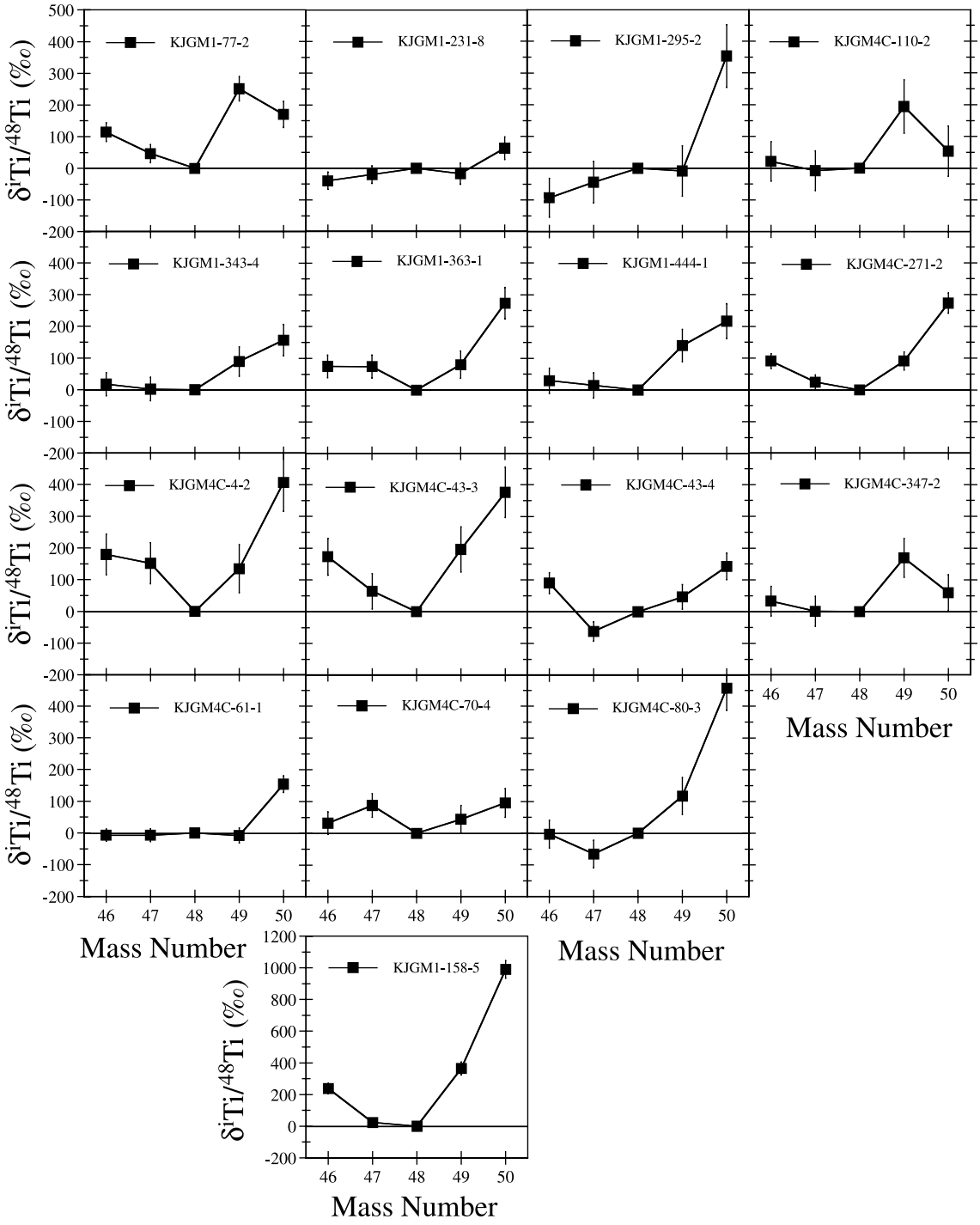

FIG. 4.—Titanium isotopic patterns in Y grains with greater than 2 σ anomalies in at least one Ti isotopic ratio. Note that the Y-axis scale for grain KJGM1-158-5 differs from those of all the other grains.

required for the condensation of SiC grains and other carbonaceous phases (Larimer 1968; Sharp & Wasserburg 1995; Lodders & Fegley 1997).

The isotopic compositions of the CNO elements in the envelope are also strongly affected by previous H burning during the main-sequence phase and subsequent first and second (only for $M \gtrsim 3.5\ M_{\odot}$ stars) dredge-up (Iben 1977; Dearborn 1992; El Eid 1994; Boothroyd & Sackmann 1999). During the first dredge-up, the convective envelope penetrates into deep regions, where some proton captures occurred on CNO nuclei during the main sequence, partially destroying ^{12}C and producing a layer enriched in ^{13}C. As a result, the initial $^{12}C/^{13}C$ ratio ($=89$ for a solar composition) of the envelope drops to a canonical value of ~ 25, independent of mass and metallicity (Iben 1977). According to spectroscopic observations (Lambert 1981; Sneden, Pilachowski, & Vandenberg 1986; Gilroy 1989; Gilroy & Brown 1991; Wallerstein & Morell 1994), in low-

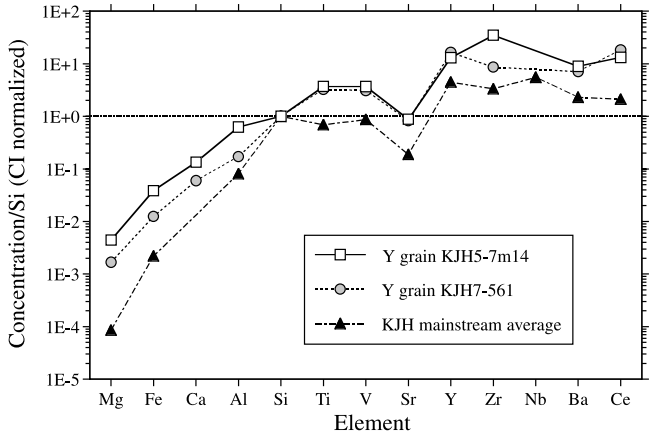

FIG. 5.—Trace element abundances measured in two Y grains are compared with the averages of KJH mainstream grains (Amari et al. 1995). The abundances are normalized to Si and the solar system abundances (Anders & Grevesse 1989). See the electronic edition of the Journal for a color version of this figure.

mass ($M < 2.3\ M_\odot$) red giants of Galactic disk metallicity there is a further drop in the $^{12}C/^{13}C$ ratio by approximately a factor of 2 before the early AGB phase. This observation has been interpreted as the consequence of extra mixing (e.g., Iben & Renzini 1984), subsequently called cool bottom processing (CBP, Wasserburg, Boothroyd, & Sackmann 1995), possibly induced by rotational shear instabilities (Charbonnel 1995; Charbonnel, Brown, & Wallerstein 1998). The second dredge-up occurs in intermediate-mass stars of $M \gtrsim 3.5\ M_\odot$, and mixes some extra ^{14}N and ^4He from the He core into the envelope. The C isotopic ratio of the envelope is thus determined by nucleosynthesis during the main-sequence and red giant stages as well as during the AGB phase (Iben 1977; Bazan 1991; Gallino et al. 1994). In contrast, the envelope $^{14}N/^{15}N$ ratio is not significantly modified during the AGB phase.

One exception occurs in stars more massive than $5\ M_\odot$, which experience hot bottom burning (HBB). This process, H burning in the CN cycle, occurs in the very deep layers of the convective envelope at high enough temperature ($\sim 60 \times 10^6$ K). Carbon-12, including the newly synthesized ^{12}C dredged up from the He intershell, is converted into ^{13}C and ^{14}N. As a consequence, the $^{12}C/^{13}C$ ratio drops to near its equilibrium value of ~ 3.5 and the C/O ratio decreases to a few tenths. The $^{14}N/^{15}N$ greatly increases, to $20–30 \times 10^3$. According to Lattanzio et al. (1996), and Lattanzio & Forestini (1999), loss by stellar winds causes the convective envelope to retreat, HBB ceases, and the C/O and $^{12}C/^{13}C$ ratios eventually increase because of TDU. In the models by Lattanzio & Forestini (1999), a $6\ M_\odot$ AGB star of solar metallicity remains O-rich, while it becomes C-rich for metallicities $Z = 0.004$ and 0.008, typical of Magellanic Cloud stars. However, the $^{12}C/^{13}$ C ratio does not increase to values larger than ~ 12.

Whereas the C and N isotopic compositions of mainstream grains are completely dominated by nucleosynthesis occurring in the parent stars, this does not appear to be the case for Si and Ti. Although the isotopic ratios of these two elements *are* predicted to be modified by neutron capture and TDU in AGB stars (Gallino et al. 1994; Lugaro et al. 1999), single grain studies (Zinner et al. 1989; Stone et al. 1991; Virag et al. 1992; Alexander 1993; Hoppe et al. 1994; Huss et al. 1997; Alexander & Nittler 1999) have shown that the grains' compositions cannot be explained in terms of the *s* process in AGB stars only and apparently reflect also the initial compositions of the parent stars (Clayton et al. 1991; Alexander 1993). The diverse original isotopic compositions have been interpreted to be the result of the Galactic chemical evolution of the Si isotopes (Gallino et al. 1994; Timmes & Clayton 1996; Clayton & Timmes 1997; Alexander & Nittler 1999) and/or of additional heterogeneous mixing of SN ejecta into the ISM (Lugaro et al. 1999).

The isotopic compositions of elements heavier than Fe in SiC are dominated by *s*-process nucleosynthesis (Hoppe & Ott 1997; Gallino et al. 1997). In fact, it is the close agreement between the measured isotopic patterns of the heavy elements (see, e.g., Hoppe & Ott 1997; Zinner 1998) with theoretical models of nucleosynthesis in AGB stars (Gallino et al. 1997), which constitutes the most convincing argument for an AGB origin of the mainstream SiC grains.

4.1.1. *Silicon and Titanium Isotopic Ratios in Mainstream Grains*

Before discussing the Si and Ti isotopic ratios in Y grains we want to briefly review the Si and Ti isotopic compositions of mainstream grains. Figure 2 shows the Si isotopic ratios of KJG mainstream grains. They and the data for SiC from other Murchison size fractions (Hoppe et al. 1994, 1996b) and other meteorites (Stone et al. 1991; Alexander 1993; Huss et al. 1997) are spread along a line of slope 1.31, the "mainstream correlation line." Lugaro et al. (1999) argued that mainstream grains most likely come from AGB stars with masses between 1.5 and $3\ M_\odot$ and with solar metallicity. Neutron-capture reactions in such stars are predicted to shift the original $^{29}Si/^{28}Si$ on average by 20‰ and the $^{30}Si/^{28}Si$ ratio on average by 25‰ (Lugaro et al. 1999, see their Fig. 5). These values imply that the original Si isotopic compositions of the parent stars plot along a slope-1.31 line with a $\delta^{29}Si/^{28}Si$ value of -3.2‰ at the intercept at $\delta^{30}Si/^{28}Si = 0$. The average $\delta^{29}Si/^{28}Si$ value of the thus-adjusted initial Si isotopic ratios inferred for the parent stars is shifted from 50.4‰ to 30.4‰.

The Galactic chemical evolution models of the Si isotopes by Gallino et al. (1994), Timmes & Clayton (1996), and Alexander & Nittler (1999) assumed a monotonic increase of the $^{29}Si/^{28}Si$ and $^{30}Si/^{28}Si$ ratios in the ISM with increasing metallicity. The reason for this behavior is that ^{28}Si is a primary isotope, i.e., it is produced in stars starting only with H and He. In contrast, ^{29}Si and ^{30}Si are secondary isotopes: they are produced in stars starting from seeds derived from previous stellar generations. In the Galactic evolution models the "AGB-corrected" correlation line of the Si isotopes represents the average compositions of stars of varying ages and/or metallicities. We shall call this line also the "Galactic line" since it represents the Galactic (parent star) component of the isotopic compositions of the grains. However, as argued by Alexander & Nittler (1999) and explicitly modeled by Lugaro et al. (1999), this line probably has a certain width due to heterogeneous mixing during Galactic evolution. Lugaro et al. (1999) interpreted the Si isotopic distribution of the mainstream grains as originating from heterogeneities of the material from which the parent stars of the mainstream grains formed. In this interpretation the Si isotopic composition of the ISM at any Galactic time is given as a distribution rather than a

unique value as assumed in other Galactic evolution models (Timmes, Woosley, & Weaver 1995; Timmes & Clayton 1996; Alexander & Nittler 1999) and in this way could successfully explain the slope of 1.31 for the mainstream correlation line. For the rest of this paper we shall call the Si isotopic ratios of the grains due to the compositions of their parent stars "Galactic component" or "Galactic evolution component," irrespective of whether local heterogeneities or a monotonic temporal evolution of the ISM isotopic abundances is the dominant mechanism.

Hoppe et al. (1994) noticed that the Ti and Si isotopic ratios in mainstream SiC grains are correlated. In Figures 6*a*–6*d* we show the Ti isotopic ratios plotted versus the $^{29}Si/^{28}Si$ ratio of the KJH mainstream grains measured by Hoppe et al. (1994) and the set of MUR grains analyzed by Alexander & Nittler (1999). Although far from being perfect, there is a general correlation between the Ti and Si isotopic ratios. In this figure we also show the best-fit lines to the data points. As in the case of Si, the Ti isotopic variations among mainstream grains cannot be solely accounted for by *s*-process nucleosynthesis in AGB stars. This is especially apparent for the two light isotopes: $\delta^{46}Ti/^{48}Ti$ and $\delta^{47}Ti/^{48}Ti$ values measured in the grains range up to $\sim 200‰$ and 100‰, respectively, whereas the maximum predicted change from TDU, for AGB stars of mass 1.5 and 3 $M_\odot$, is 50‰ for $^{46}Ti/^{48}Ti$ and 12‰ for $^{47}Ti/^{48}Ti$ (Lugaro et al. 1999). Furthermore, the correlation with the Si isotopic ratios also implies that the Ti ratios of the grains are dominated by the original isotopic compositions of the parent stars. We note that the two most abundant isotopes, ^{28}Si and ^{48}Ti, used as reference isotopes for the Si and Ti isotopic ratios, are of primary origin. Both show a very similar behavior in halo stars where the synthesized matter derives only from the ejecta of massive Type II supernovae (SNe II) (e.g., Wheeler, Sneden, & Truran 1989; Gratton & Sneden 1994; Timmes et al. 1995). Consequently, the general Si-Ti correlation exhibited by mainstream SiC grains indicates that ^{46}Ti and ^{47}Ti, similar to ^{29}Si and ^{30}Si, behave as secondary isotopes. This is in general agreement with the Woosley & Weaver (1995) calculations for the yields from SNe II of different metallicity (see also Timmes et al. 1995 for a Galactic evolution model of the Ti isotopes).

Above we subtracted the average predicted AGB contribution from the grains' Si isotopic ratios to infer the original ratios of the parent stars, and it seems reasonable to do the same thing to obtain the initial Ti isotopic ratios. However, this is much more uncertain. One reason is that predicted shifts are larger for Ti (especially for the $^{49}Ti/^{48}Ti$ and $^{50}Ti/^{48}Ti$ ratios) than for Si, another reason is the fact that the main neutron source responsible for the *s*-process modification of Si in AGB stars is ^{22}Ne, whereas the ^{13}C source plays an important role for the production of ^{50}Ti (Lugaro et al. 1999). This means that the predicted shifts in Si isotopic ratios do not depend much on the amount of ^{13}C assumed to be present in the intershell region where radiative burning produces neutrons (see Fig. 5 of Lugaro et al. 1999). In contrast, predicted shifts for the $^{50}Ti/^{48}Ti$ ratio vary considerably with the amount of ^{13}C (see Figs. 5 and 6 of Lugaro et al. 1999). The intershell ^{13}C abundance is a priori not well constrained, and a large range is required to explain the scatter of the abundances of *s*-elements in *s*-enriched stars, even for stars of the same metallicity (Busso et al. 2000). A range in the strength of the ^{13}C pocket implies large uncertainties in predicted $^{50}Ti/^{48}Ti$ ratios. Plotted in Figures 6*a*–6*d* as gray bands are the compositions we obtain after subtracting from the correlation lines the theoretically predicted shifts for 1.5 and 3 $M_\odot$ stars of solar metallicity with the three choices of the ^{13}C abundance (d3, ST, and u2) given in Figures 5 and 6 of Lugaro et al. (1999). As can be seen from the graphs, the "AGB-corrected" correlation line of $^{50}Ti/^{48}Ti$ versus $^{29}Si/^{28}Si$ has very large uncertainties. These uncertainties can, in principle, account for the spread of the data points in the $^{50}Ti/^{48}Ti$ versus $^{29}Si/^{28}Si$ plot. However, the uncertainty expressed by the wide gray band is the lack of our knowledge about the Galactic line and does not necessarily mean that the Galactic component itself does have such a wide distribution. In the other plots, especially $^{46}Ti/^{48}Ti$ and $^{47}Ti/^{48}Ti$ versus $^{29}Si/^{28}Si$, the scatter of the mainstream SiC data points around the correlation line is greater than the uncertainties in the AGB contributions. In these cases this extra scatter probably reflects the intrinsic distribution of the Ti isotopic compositions of the ISM due to heterogeneities in the SN contributions, similar to what has been proposed for the Si isotopes by Lugaro et al. (1999). However, a quantitative treatment of this problem is still outstanding. In contrast to the Si isotopes, for the Ti isotopes we do not know the width of the Galactic line.

Another unsettling feature of the Ti data is the following: whereas the "AGB-corrected" correlation line essentially goes through the solar Si isotopic composition, the corrected Ti-Si lines miss the solar composition by large amounts for the $^{49}Ti/^{48}Ti$ and $^{50}Ti/^{48}Ti$ isotopic ratios (see Figs. 6*c* and 6*d*). If, as seems to be indicated by the mainstream grains, the Galactic line for Si isotopes goes through the solar composition, the "Galactic" $^{49}Ti/^{48}Ti$ and $^{50}Ti/^{48}Ti$ isotopic ratios differ from the solar ratios by 110‰–140‰ and 80‰–360‰, respectively. This discrepancy might in part be due to large uncertainties in the neutron-capture cross sections for the Ti isotopes (see Table 1 of Lugaro et al. 1999); however, the AGB shifts for these two isotopes would have to be essentially zero for the Galactic line to pass through the solar composition. What makes the issue even more uncertain is the fact that Ti measurements on finer-grained bulk samples of SiC give higher $^{50}Ti/^{48}Ti$ ratios than the single grain measurements (see the results of Ti isotopic measurements in bulk samples by Amari, Zinner, & Lewis 2000b). Still, the single grain data seem to indicate that the solar system had an anomalous Ti isotopic composition at least for the $^{49}Ti/^{48}Ti$ and $^{50}Ti/^{48}Ti$ ratios (see Figs. 6*c* and 6*d*) compared to the composition of the ISM as inferred from the mainstream grains and theoretical AGB shifts. In Figures 6*e*–6*h* we add for comparison the Y grain to the mainstream data but leave out the mainstream correlations lines and plot only one set of inferred AGB-corrected correlation lines (for the standard model ST see § 4.2.2).

4.2. *Y Grains*

The characteristic properties of Y grains that distinguish them from mainstream grains are their larger $^{12}C/^{13}C$ ratios (Fig. 1) and their Si isotopic compositions, which plot to the right of the mainstream correlation line (Fig. 2). On the other hand, the N isotopic and the $^{26}Al/^{27}Al$ ratios are in the same range as those of mainstream grains. This suggests that the Y grains also originated from C-rich AGB stars, but they are more enriched in the products of He burning (^{12}C) and the *s* process than the mainstream grains.

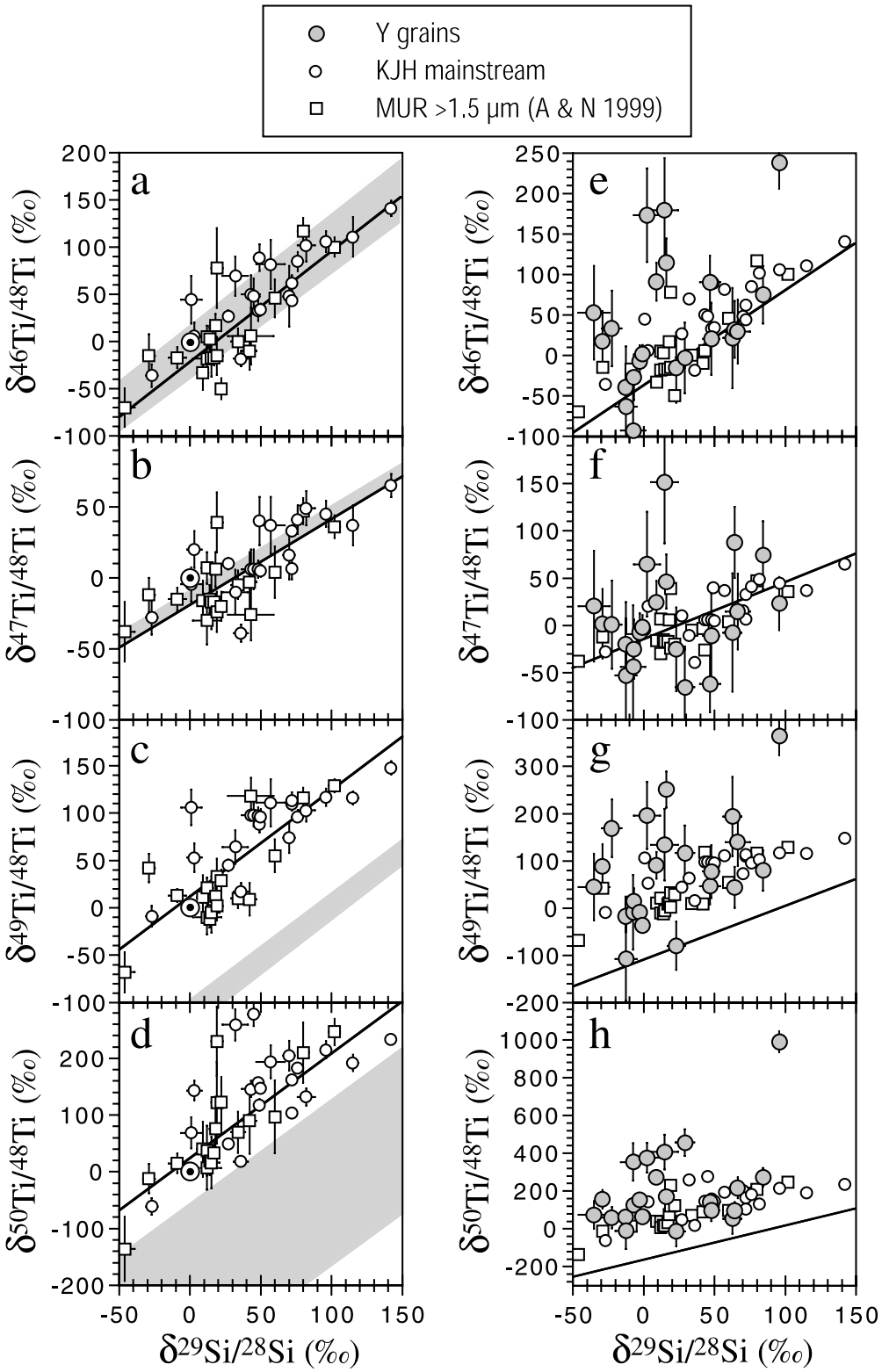

FIG. 6.—(*a–d*) Titanium isotopic ratios of mainstream grains (Hoppe et al. 1994; Alexander & Nittler 1999) are plotted against their $^{29}Si/^{28}Si$ ratios. The solid lines are the best-fit lines to the data points. The gray bands are the isotopic compositions inferred for the parent stars of the grains ("Galactic component") if the theoretical contributions of AGB neutron-capture synthesis are subtracted from the grains' isotopic ratios. The $^{50}Ti/^{48}Ti$ ratios predicted for the envelope of AGB stars sensitively depends on the assumed ^{13}C pocket responsible for neutron production in the He intershell (Lugaro et al. 1999), resulting in large uncertainties for the Galactic component. (*e–h*) Same as figure (*a–d*) but with the Y grain data of this study added to the plot. To avoid clutter only the errors of the Y grains are plotted. Note that in order to accommodate the Y grain data, the range of the plots has been increased. The lines are the Galactic lines inferred from the standard (ST) ^{13}C pocket for the AGB nucleosynthesis in 1.5 and 3 $M_{\odot}$ stars of solar metallicity.

In fact, Hoppe et al. (1994) proposed that the six Y grains of their study formed in a single AGB star, since they lie on a line of a slope of 0.35 in a Si 3-isotope plot, similar to the slope predicted for neutron capture in a single AGB star of solar metallicity. The 27 Y grains of this work and the other grains of Hoppe et al. (1994) with $^{12}C/^{13}C > 100$ do not all lie on this single line and, if they have an AGB origin, must come from several stars with different initial Si isotopic compositions. However, most of them do lie fairly close to the original Y-grain line, indicating a narrower range of initial Si isotopic compositions than mainstream grains.

Lodders & Fegley (1998) proposed CH stars as a stellar source of Y grains. There are two subgroups of CH stars. Stars of the first group have low $^{12}C/^{13}C$ ratios (<10) and metallicities Z between 0.01 and 0.1 $Z_\odot$. Many such stars occur in binary systems. Stars of the second group have, in contrast, very high $^{12}C/^{13}C$ ratios (≥ 90) and are also extremely metal-depleted ($Z < 0.003$). They have large enrichments of *s*-process elements. These stars do not occur in binaries and are considered to be the Population II counterparts of C (N-type) stars of Population I. There are only very few isotopic data available for CH stars and no detailed nucleosynthesis calculations to check this proposal have been performed. However, CH stars of this class are strongly enriched in α-elements, which means that they probably are overabundant in ^{28}Si and ^{48}Ti relative to the other Si and Ti isotopes. This and their low metallicity suggest that they have lower than solar $^{29,30}Si/^{28}Si$ and $^{46,47}Ti/^{48}Ti$ ratios (Timmes et al. 1995) and argue against a CH origin of Y grains.

In any case, here we shall assume that AGB stars are the source of Y grains and investigate the implications of this assumption. As has been shown in Figure 1, the $^{14}N/^{15}N$ and inferred $^{26}Al/^{27}Al$ ratios in Y grains do not differ from those in mainstream grains. The envelope $^{14}N/^{15}N$ ratio is not significantly affected by nucleosynthesis in most AGB stars (but see discussion of HBB above). While ^{26}Al is produced during the TP-AGB phase, apparently the conditions affecting its production are very similar in the parent stars of mainstream grains and Y grains. We shall therefore concentrate on a detailed comparison of only the Si and Ti isotopic ratios with AGB models.

4.2.1. *Silicon Isotopic Ratios in Y Grains*

A key observation is that the Si isotopic shifts predicted from AGB nucleosynthesis for 1.5 and 3 $M_\odot$ stars of solar metallicity (see Fig. 5 of Lugaro et al. 1999) cannot account for the deviations of the Si isotopic ratios of the Y grains from the mainstream correlation line (Fig. 2). However, AGB stars of higher mass or of lower metallicity can produce the larger shifts of the Y grains (see Figs. 7 and 8 of Lugaro et al. 1999). Here we assume that, as for the mainstream grains, the Si isotopic compositions of the Y grains can be explained by two components: the Galactic component, representing the compositions of the parent stars, and the AGB component. We furthermore assume that the initial Si isotopic compositions of the parent stars of the Y grains plot on the same line as those of the mainstream grains. With these assumptions we can determine the initial compositions of these stars by projecting the Y grains' compositions onto this line, the AGB-corrected correlation line of the mainstream grains, along a slope 0.5 line. This is the slope of the evolution of the Si isotopes in a 5 $M_\odot$ star of solar metallicity or in a 3 $M_\odot$ star of metallicity $Z = 0.006$ (Lugaro et al. 1999). The results are shown in Figure 7. It is apparent from the plot that the projected compositions of most of the Y grains have negative $\delta^{29}Si/^{28}Si$ and $\delta^{30}Si/^{28}Si$ values, in contrast to the ratios of most mainstream grains. The average inferred initial $\delta^{29}Si/^{28}Si$ and $\delta^{30}Si/^{28}Si$ values of the Y grain parent stars are $-28.8‰$ and $-19.6‰$ (with standard deviations of 39.4‰ and 30.1‰), respectively, whereas those of the mainstream grains are 30.4‰ and 26.6‰ (standard deviations 42.7‰ and 30.6‰) (Lugaro et al. 1999). If the average $^{29}Si/^{28}Si$ and $^{30}Si/^{28}Si$ ratios of stars increase with metallicity (Timmes & Clayton 1996), this indicates that the parent stars of the Y grains had lower metallicities than those of the mainstream grains.

Of course it is not said that the parent star compositions of the Y grains have to lie on exactly the same line as the ratios of the mainstream grain parent stars and even the assumption that they lie on a single line is an oversimplification. Indeed, we do not know along which line in the Si 3-isotope plot the average composition of the Galaxy evolves. If it evolves along a line with slope 1, as for example in the Timmes & Clayton (1996) model, we would have to project the Y grain data either onto this line (in case the Galaxy has a unique composition at any given time) or onto a line with slope 1.31 but shifted to the left of the AGB-corrected mainstream line. However, the results would not be very different and the conclusion that the initial parent star compositions of the Y grains were isotopically lighter and these stars therefore were of lower metallicity would remain valid.

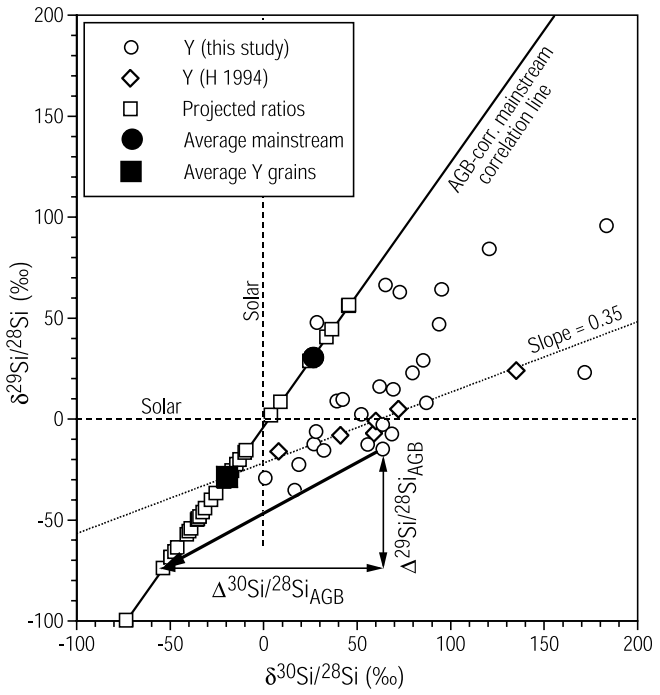

FIG. 7.—Si isotopic compositions of the Y grains are projected onto the AGB-corrected mainstream correlation line along lines of slope 0.5. The AGB-corrected mainstream correlation line is assumed to represent also the initial Si isotopic ratios of the Y grains' parent stars and the slope 0.5 lines to represent the evolution of the Si isotopes in the envelope of low-metallicity AGB stars. The quantities $\Delta^{29}Si/^{28}Si$ and $\Delta^{30}Si/^{28}Si$ thus are the assumed shifts in the Si isotopic ratios due to AGB nucleosynthesis only. Plotted as large solid symbols are the average inferred compositions of the parent stars of the mainstream and type Y grains. See the electronic edition of the Journal for a color version of this figure.

In Figure 7 we indicate by an arrow the shift from the original composition to the mainstream line. If our assumptions (that there are two components contributing to the Si isotopic composition of each grain and that the line representing the Galactic component and the slope of the AGB evolution describe reality) are correct, this shift is the AGB modification of the isotopic ratios of the Y grains. To compare the grain data with theoretical models of AGB nucleosynthesis, we therefore will use the horizontal component of the shifts, $\Delta^{30}Si/^{28}Si_{AGB}$, as shown in the figure. The models we shall compare the grain data to are the same as those described by Lugaro et al. (1999) except that they encompass a larger range of masses and metallicities. There are several uncertainties in this comparison. If local heterogeneities are the cause of the Si isotopic distribution along the mainstream line, the Monte Carlo (MC) model of Lugaro et al. (1999) shows that this distribution, which extends mostly along the line, has also a certain scatter around the line. This scatter would add an error to $\Delta^{30}Si/^{28}Si_{AGB}$. We have performed a MC calculation similar to the ones by Lugaro et al. (1999) to reproduce the distribution of the Si isotopic ratios of the Y grains projected onto the AGB-corrected mainstream correlation line (Fig. 7, *open squares*). The standard deviation of the distance along the $\delta^{30}Si/^{28}Si$ direction from the best-fit line to the Si distribution produced by the MC simulation was found to be $\sim 11‰$. This is very similar to the standard deviation in $\delta^{30}Si/^{28}Si$ of the mainstream grain Si isotopic compositions from the mainstream correlation line (11.7‰). While these values are somewhat larger than the experimental uncertainties for the Y grains' Si isotopic ratios, they are still smaller than the systematic uncertainty that arises from the fact that we do not know the exact composition of the "Galactic component." However, this uncertainty constitutes a systematic error and would not affect the individual data points in a random way.

It should be mentioned that an additional uncertainty arises from the fact that the $\delta^{29}Si/^{28}Si$ versus $\delta^{30}Si/^{28}Si$ lines for the AGB contributions can have different slopes. We assumed a slope of 0.5 but the models for $Z = 0.01$ stars discussed below that can account for the large Si isotopic shifts observed in the grains give slopes between 0.43 and 0.55 for different masses and stellar models. To assess the uncertainties in $\Delta^{30}Si/^{28}Si_{AGB}$ resulting from different slopes we calculated the shifts for the two extreme slopes 0.43 and 0.55. The resulting uncertainties depend on the distance of the data points from the Galactic line. The average for all Y grains is 6.1‰ with a maximum of 18‰ for grain KJGM1-337-3, the grain farthest from the Galactic line. To obtain the total errors of the $\Delta^{30}Si/^{28}Si_{AGB}$ values we combined the individual measurement errors, the width of the Galactic line and the uncertainties resulting from the range in the slope of the AGB evolution line.

Figure 8 shows a graph of the $\Delta^{30}Si/^{28}Si_{AGB}$ shifts plotted against the $^{12}C/^{13}C$ ratios measured in the Y grains. These grain data are compared to theoretical predictions for the envelopes of AGB stars of three different masses (1.5, 3, and 5 $M_\odot$) and three different metallicities ($Z = 0.006$, 0.01, and 0.02) during TDU in the TP phase. The envelope is recurrently enriched by TDU in ^{12}C and in the heavy Si isotopes as a function of increasing number of TDU episodes. Although there is a large amount of scatter in the grain data, they show the general correlation expected from the TDU. It should be emphasized, however, that a perfect

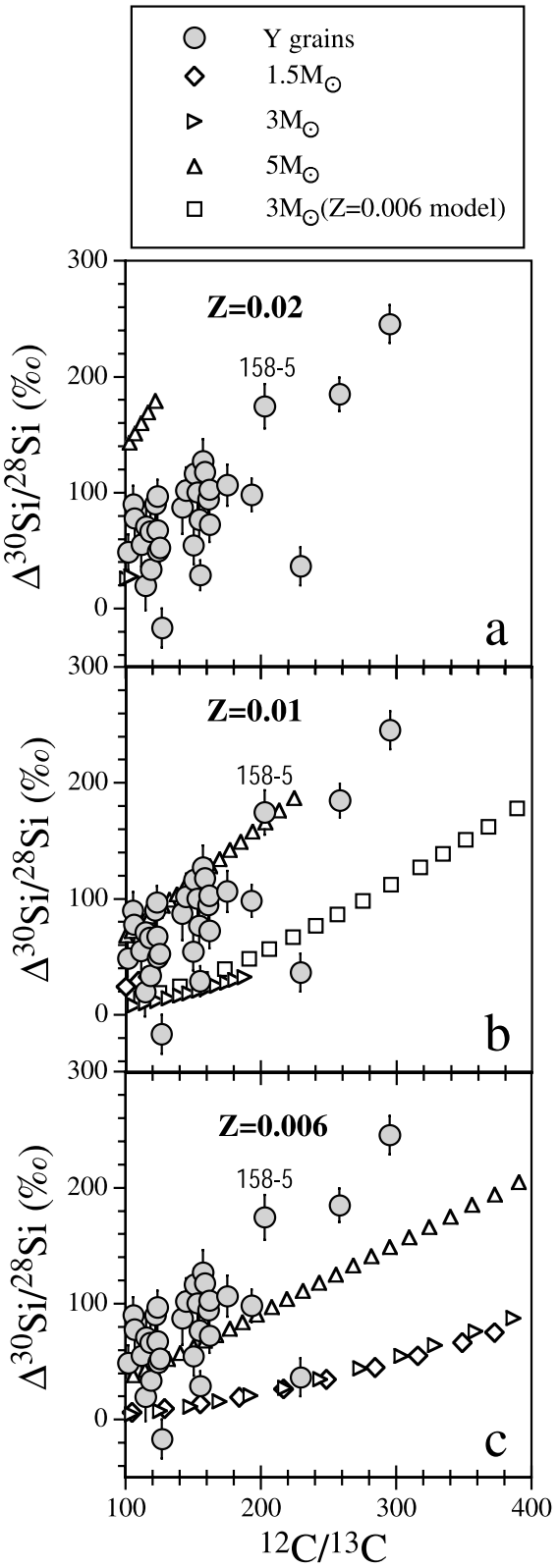

FIG. 8.—Projected shifts of Si isotopic ratios of the analyzed Y grains from the AGB-corrected mainstream correlation line are plotted vs. their $^{12}C/^{13}C$ ratios. Also plotted are model predictions for the envelope of AGB stars of varying mass and metallicity. For $Z = 0.02$ the predictions are based on three stellar FRANEC models (Straniero et al. 1997; Gallino et al. 1998). For $Z = 0.01$ the predictions are simulated, based on the solar metallicity stellar models, for 3 $M_\odot$ also on the $Z = 0.006$ stellar model. In the $Z = 0.006$ cases we used the 3 $M_\odot$ FRANEC model for this mass and simulations for the other two masses. See the electronic edition of the Journal for a color version of this figure.

correlation would be seen only if all the grains came from the same star; considerable scatter is expected if the grains came from stars with a range of masses and metallicities.

As can be seen from the plots, only stars with metallicity lower than solar reach high enough C isotopic ratios to cover those observed in the grains. The reason is that stars of lower metallicity have lower initial abundances of all metals including C and O. Addition of approximately the same amount of ^{12}C during the TDU will therefore result in higher $^{12}C/^{13}C$ (and also C/O) ratios. Furthermore, low-metallicity AGB stars dredge up more material after each thermal pulse, increasing the $^{12}C/^{13}C$ ratio even more (Wood 1981; Straniero et al. 2000). Final $^{12}C/^{13}C$ ratios also depend on stellar mass. Stars of less than 2.5 $M_\odot$ are observed to have $^{12}C/^{13}C$ ratios lower than predicted by standard models of red giant branch nucleosynthesis and mixing. These observations are believed to indicate that the lower mass stars have experienced CBP before the AGB phase, lowering the initial envelope $^{12}C/^{13}C$ ratio before the start of the TP phase. In the models plotted in Figure 8 we assumed this initial ratios for 1.5 $M_\odot$ stars to be 12, whereas a "canonical" value (without CBP) of 24 was chosen for the more massive stars.

It should be emphasized that the amount of dredge-up as derived from the FRANEC models used here is in strict agreement with astronomical observations and with the C and Si isotopic composition of the mainstream grains. For example, Alexander & Nittler (1999) used a phenomenological approach to mix He-shell material into the envelope (see their Fig. 4). If one does not set limits to the dredged-up mass, one can reach large $^{12}C/^{13}C$ and $\Delta^{30}Si/^{28}Si$ values, in principle as high as those observed in the Y grains. We have doubled the standard mass dredged up in the 1.5 $M_\odot$ model of solar metallicity and found that the maximum values reached for $^{12}C/^{13}C$ and $\Delta^{30}Si/^{28}Si$ are approximately twice those of the standard case. However, the maximum C/O ratio reached is 2.6, significantly higher than the range of 1–1.5 observed in Galactic disk carbon stars of essentially solar compositions (Lambert et al. 1986; Smith & Lambert 1990). Furthermore, the distribution of $^{12}C/^{13}C$ ratios in mainstream grains agrees very well with those observed in carbon stars (Lambert et al. 1986; Dominy & Wallerstein 1987; Smith & Lambert 1990). The range of $\sim$30–70 is much lower than the ratios predicted for AGB stars of solar metallicity if the dredge-up mass is increased (for example, the maximum $^{12}C/^{13}C$ ratio for the 1.5 $M_\odot$ model of solar metallicity with double dredge-up would be 116). Finally, the Si isotopic compositions of mainstream grains (Fig. 2) do not indicate large shifts (as long as the initial Si isotopic distribution included the solar system values). For all these reasons it appears extremely unlikely that the third dredge-up in solar metallicity AGB stars is much higher than what we deduced from the FRANEC models and that solar metallicity carbon stars could account for the C and Si isotopic ratios of Y grains. Of course, Y grains are a rare population and we cannot rule out that some unknown process leads to anomalously high TDU in a small fraction of solar metallicity AGB stars. However, since no such process has been identified, the results shown in Figure 8 suggest an origin in $Z < Z_\odot$ AGB stars for the Y grains is much more likely.

The modification of the Si isotopic ratios predicted for AGB star envelopes due to neutron capture also depends on metallicity. The temperature of the He shell in low-metallicity stars is slightly higher than in stars of solar metallicity, enhancing the heavy Si isotope abundances. In addition, the strength of the TDU in stars with $Z = 0.006$ is approximately twice that in stars of solar metallicity (Gallino et al. 1998). The initial Si isotopic ratios in the AGB models were assumed to be solar, even for stars with lower than solar metallicity. There is a certain inconsistency in this assumption but we do not expect that solar starting ratios will make much difference in the *s*-process effects on the Si isotopes for the comparisons with the Y grain ratios. First, the AGB-corrected average $^{29}Si/^{28}Si$ ratio of the Y grains, presumably reflecting the initial ratio of their parent stars, is only 3% smaller than the solar ratio and 6% smaller than the average of the mainstream grains (see Fig. 7). Second, we compare shifts of isotopic ratios, which in first order are independent of the initial Si ratios as long as these are not vastly different.

While we confidently can exclude stars of solar metallicity as sources of the Y grains, stars with a metallicity of $Z = 0.006$ also are unlikely sources. While their predicted $^{30}Si/^{28}Si$ ratios cover the range observed in the grains, their predicted $^{12}C/^{13}C$ ratios reach much higher values (373 for the 1.5 $M_\odot$, 637 for the 3 $M_\odot$, and 780 for the 5 $M_\odot$ model) than those measured in the grains. Furthermore, the theoretical slope of the $\Delta^{30}Si/^{28}Si$ versus $^{12}C/^{13}C$ correlation is too small for the 1.5 and 3 $M_\odot$ stars and misses most of the grain data. Only the 5 $M_\odot$ model covers some of the data points. However, a 5 $M_\odot$ $Z = 0.006$ star is likely to experience hot bottom burning (HBB) that drastically lowers the $^{12}C/^{13}C$ and C/O ratio. In the model by Lattanzio & Forestini (1999) a 5 $M_\odot$ star undergoes HBB already at solar metallicity and even more pronounced HBB at lower metallicities (typical of Magellanic Cloud stars). With the FRANEC code used to calculate the AGB models discussed here (Straniero et al. 1997; Gallino et al. 1998), we do not see HBB in the 5 $M_\odot$ model with $Z = 0.02$ but we do see it in the 6 $M_\odot$ model and in the 5 $M_\odot$ model with $Z = 0.01$ (Straniero et al. 2000).

Stars of metallicity $Z = 0.01$ with masses between 3 and 5 $M_\odot$ have predicted envelope compositions that cover most of the C and Si isotopic compositions of the grains. It should be mentioned that we have full stellar evolution models only for the three stars with solar metallicity and for the 3 $M_\odot$ star of metallicity $Z = 0.006$. Nucleosynthesis calculations for the other cases were simulated based on the results of the solar metallicity models. For the 3 $M_\odot$ star of $Z = 0.01$ we used both the $Z = 0.02$ and $Z = 0.006$ stellar models and the results for both are plotted in Figure 8*b*. There is a substantial difference between them, the maximum $^{12}C/^{13}C$ ratio is 188 if the solar model is used but reaches 389 if the $Z = 0.006$ model is used. This is because the efficiency of the TDU is typically doubled in our 3 $M_\odot$ $Z = 0.006$ evolutionary model compared to the solar metallicity model. It is clear that a full stellar evolution model with $Z = 0.01$ will yield intermediate results between the $Z = 0.02$ and $Z = 0.006$ stellar models we used for the nucleosynthesis calculations. We also expect that results of a full stellar model with 5 $M_\odot$ and $Z = 0.01$ will differ somewhat from the predictions of the simulation plotted in Figure 8*b*, toward higher $^{12}C/^{12}C$ and $^{30}Si/^{28}Si$ ratios.

We have to await the availability of a wider range of models to make more detailed quantitative comparison, but the picture is already quite clear. On the basis of the C and

Si isotopic data we can conclude that AGB stars with metallicities around half of solar are the most likely sources of the Y grains. Unfortunately, the data do not set very strong constraints on the masses of the Y grain parent stars. A range of masses and metallicities is obviously required to accommodate all the grain data and the grains with the highest $\Delta^{30}Si/^{28}Si$ values appear to require parent stars of intermediate mass (i.e., with $M > 3\ M_{\odot}$). Of course, there are considerable uncertainties in the models. For example, if the initial $^{12}C/^{13}C$ ratio before the beginning of the TP-AGB phase is assumed to be 12 instead of 24 for the 3 $M_{\odot}$, $Z = 0.01$ case, then these stars would cover most of the Y grain data points in Figure 8*b*. Although $3M_{\odot}$ stars of solar metallicity are not expected to experience cool bottom processing, such extra mixing is conceivable for intermediate-mass stars of lower metallicity (Boothroyd & Sackmann 1999). Another possibility is that the rate of the reaction $^{22}Ne(\alpha, n)^{25}Mg$, responsible for the production of neutrons in the convective pulse, is higher than assumed. This would increase the production of the heavy Si isotopes and thus increase $\Delta^{30}Si/^{28}Si$ in Figure 8. Finally, there are still considerable uncertainties in the neutron-capture cross sections affecting the Si isotopes (see Table 1 of Lugaro et al. 1999).

4.2.2. *Titanium Isotopic Ratios in Y Grains*

If we want to compare the Ti isotopic compositions of Y grains with models of AGB nucleosynthesis, we are faced with the same problem we encountered with the Si isotopes, namely that in order to obtain the Ti isotopic shifts due to AGB nucleosynthesis we have to correct for the Galactic contribution to the isotopic ratios. For the case of Si, we calculated the shifts of the Y grain ratios relative to the AGB-corrected mainstream line and assumed that these shifts represent the AGB contributions. If we consider the problem in full generality, we should in fact combine the Si and Ti isotopic compositions. We thus consider the six-dimensional space spanned by the two Si and four Ti isotopic ratios. The Si and Ti isotopic composition of each Y grain is represented by a point in this space. According to our assumptions each point is arrived at from a starting composition of the grain's parent star after imposing a shift in all isotopic ratios representing the modification by AGB nucleosynthesis. The starting compositions are assumed to lie on a single line in this six-dimensional space, the Galactic line. In order to determine the AGB shifts for each grain we have to project from the measured isotopic compositions back onto the Galactic line along trajectories whose directions are determined by theoretical models of AGB nucleosynthesis.

This approach worked well for the Si isotopes only. Unfortunately, for several reasons it does not work as well for the Ti isotopes. One reason is that the measurement errors for the Ti isotopic ratios are much larger than those for the Si isotopic ratios (see Figs. 2*b* and 3 and Table 1). Another, more fundamental, reason is that, unlike for the Si isotopes, where the AGB trajectories have only a narrow range of directions (slopes in the $\delta^{29}Si/^{28}Si$ vs. $\delta^{30}Si/^{28}Si$ plane), there is a large range of directions for the Ti isotopes for models of stars with different mass and metallicity and we do not know which direction applies for a particular Y grain. We could use some average direction of the trajectory and follow this direction from the grain ratios back to the Galactic line. However, in general such a trajectory will miss the Galactic line, i.e., in the six-dimensional space of the Si and Ti isotopic ratios the two lines will not intersect. One does obtain intersects of the two lines in projections onto two-dimensional subspaces (any of the 15 combinations of the two Si and four Ti ratios) but the value of a particular ratio of the intersect point in two-dimensional plots will vary from one plot to the next. For example, in the $\delta^{29}Si/^{28}Si$ versus $\delta^{30}Si/^{28}Si$ plot the two lines will generally intersect at a different $^{29}Si/^{28}Si$ ratio than in the $\delta^{29}Si/^{28}Si$ versus $\delta^{46}Ti/^{48}Ti$ plot. To overcome this problem we could determine for each grain the point on the Galactic line that is closest to the assumed AGB trajectory. We have to define "closest" in terms of the uncertainties in the measured ratios of the grains and in the directions of the AGB trajectories for the different Si and Ti isotopic ratios. Because these uncertainties are much smaller for the Si isotopic ratios than for the Ti isotopic ratios, the "closest point" on the Galactic line, i.e., the most likely composition of the parent star of a particular Y grain, will be almost completely determined by the Si isotopic ratios of this grain.

We are therefore making only a small error if we use only the Si isotopic ratios obtained for the Galactic composition in order to determine the Ti isotopic ratios of the Galactic composition of each Y grain. To do this we used the correlations between the Ti and Si isotopic ratios in mainstream SiC grains (see our Fig. 6 and Fig. 4 of Lugaro et al. 1999) and the Galactic (AGB-corrected correlation) lines. We did so in spite of the fact that, as already mentioned earlier and as shown in Figures 6*a*–6*d*, there are large uncertainties in the thus-determined Galactic evolution lines for the Ti isotopes, especially for the $^{50}Ti/^{48}Ti$ ratio, and that some of these uncertainties reflect the original scatter of the isotopic compositions of the parent stars from the major (monotonic) Galactic evolution trend of the Ti isotopes. We considered only the standard (ST) ^{13}C pocket for the AGB models (Lugaro et al. 1999). From the mainstream Si and Ti data of Hoppe et al. (1994) and Alexander & Nittler (1999) we obtained the best-fit lines of the various Ti isotopic ratios versus the $^{29}Si/^{28}Si$ ratio. The $^{29}Si/^{28}Si$ ratio was chosen over the $^{30}Si/^{28}Si$ ratio because variations in this ratio due to the galactic component extend over a larger range. On the other hand, neutron-capture nucleosynthesis affects the $^{30}Si/^{28}Si$ ratio more than the $^{29}Si/^{28}Si$ ratio and the former was chosen for comparison of model calculations with the data (Figs. 8, 10, and 11). From the $\delta^{i}Ti/^{48}Ti$ versus $\delta^{29}Si/^{28}Si$ correlation lines we subtracted the average expected AGB contributions of 1.5 and 3 $M_{\odot}$ stars of solar metallicity (see Fig. 6 of Lugaro et al. 1999) in order to obtain four AGB-corrected correlation lines. As before, we assumed that these correlation lines represent the Galactic evolution of the Ti isotopes not only for the parent stars of the mainstream grains but also for those of the Y grains. We next used the $\delta^{29}Si/^{28}Si$ of the Y data points projected onto the AGB-corrected mainstream correlation lines of the Si isotopic ratios (the open squares in Fig. 7) to obtain projected data points on the AGB-corrected correlation lines of the Ti isotopic ratios versus the $^{29}Si/^{28}Si$ ratio. These points are assumed to represent the original isotopic compositions of the parent stars (the Galactic component) of the Y grains before they were modified by nucleosynthesis during the AGB phase. From these and the original isotopic ratios of the Y grains we calculated the projected shifts of the Ti ratios (always expressed in δ-values), which represent the change in the envelope com-

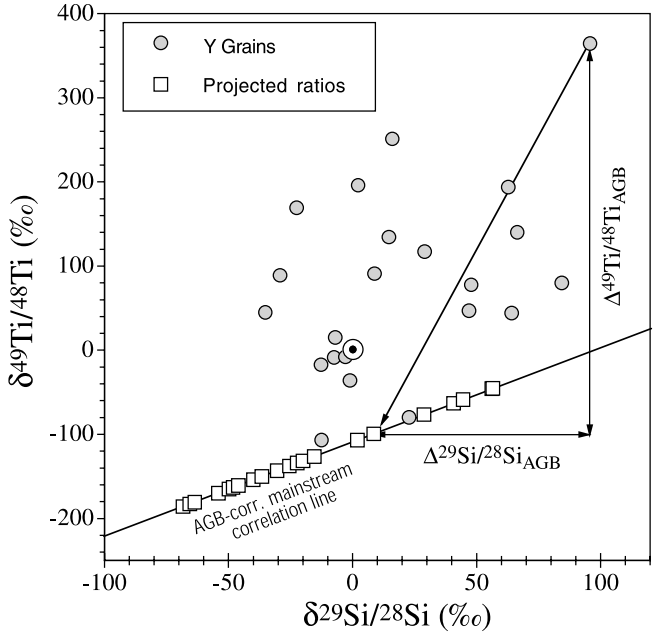

FIG. 9.—$\delta^{49}Ti/^{48}Ti$ and $\delta^{29}Si/^{28}Si$ values of the Y grains are projected onto the AGB-corrected mainstream correlation line by using the projected $\delta^{29}Si/^{28}Si$ values on the $\delta^{29}Si/^{28}Si$ vs. $\delta^{30}Si/^{28}Si$ AGB-corrected correlation line (see Fig. 7). The AGB-corrected mainstream correlation line between the Ti and Si isotopes are assumed to represent also the initial isotopic ratios of the Y grains' parent stars. From the projected compositions (*open squares*) we determine the shift in the $^{49}Ti/^{48}Ti$ ratio, $\Delta^{49}Ti/^{48}Ti_{AGB}$, assumed to represent the modification of this ratio in the parent star's envelope due to neutron-capture nucleosynthesis. A similar procedure was followed for the other isotopic ratios of Ti. See the electronic edition of the Journal for a color version of this figure.

position due to neutron-capture nucleosynthesis in the parent stars. The procedure is demonstrated for the $^{49}Ti/^{48}Ti$ ratio in Figure 9.

These shifts, denoted as $\Delta^{i}Ti/^{48}Ti$ values, together with the previously calculated $\Delta^{30}Si/^{28}Si$ values, are compared in Figure 10 to theoretical predictions of AGB models of three stellar masses and the two metallicities $Z = 0.006$ and $Z = 0.01$. As before, we have also used the slopes of 0.43 and 0.55 for the Si AGB trajectories and determined the errors of the $\Delta^{i}Ti/^{48}Ti$ values resulting from this uncertainties. These errors turned out to be small in comparison to the experimental errors; we have combined these two errors. We have also added an error expressing the width of the Galactic line. We were reluctant to just take the scatter of the mainstream data points around the $\delta^{i}Ti/^{48}Ti$ versus $\delta^{29}Si/^{28}Si$ correlation lines because varying AGB contributions, especially to the $^{49}Ti/^{48}Ti$ and $^{50}Ti/^{48}Ti$ ratios, could substantially contribute to this scatter. We therefore took values determined from the width in the Si correlation line (see § 4.2.1.) and the slopes of the $\delta^{i}Ti/^{48}Ti$ versus $\delta^{29}Si/^{28}Si$ correlation lines. The errors in Figure 10 do not include the uncertainties resulting from the lack of our knowledge of the subtracted AGB component (mostly the effect of the ^{13}C pocket) for the "Galactic component" determination. As already argued before, this is a systematic error and would shift all the Y grain data points in a given plot of Figure 10 up and down by the same amount.

Because the C and Si isotopic ratios of the grains seem to rule out solar metallicity stars as the sources of Y grains, we do not plot the Ti predictions for this case. In Figure 10*b* we plot again the predictions for the 3 $M_{\odot}$, $Z = 0.01$ star on the basis of the $Z = 0.02$ and $Z = 0.006$ model. All models plotted in Figure 10 fail to account for the large $\Delta^{46}Ti/^{48}Ti$ values observed in the grains. This is also true for the $\Delta^{47}Ti/^{48}Ti$ values but here the deviations are only slightly larger than the errors (1 σ errors are plotted). For $\Delta^{49}Ti/^{48}Ti$, the range of most of the grain data is covered by the models. However, for the models with $Z = 0.006$, high enough $\Delta^{49}Ti/^{48}Ti$ and $\Delta^{30}Si/^{28}Si$ values are reached only for $^{12}C/^{13}C$ ratios in excess of 300, the highest ratio measured in the grains. In contrast, the $Z = 0.01$ models can explain all measured compositions except for the extreme grain KJGM1-158-5, whose ratios are reached only for $^{12}C/^{13}C > 300$. For the $\Delta^{50}Ti/^{48}Ti$ ratio, the situation is similar: the $Z = 0.01$ model reproduces the grain data more easily than the other metallicities except for KJGM1-158-5, which again requires $^{12}C/^{13}C$ ratios greater than 300 in the models to account for its $\Delta^{50}Ti/^{48}Ti$ and $\Delta^{30}Si/^{28}Si$ ratios. It is clear that this is a very unusual grain. It has the largest $\delta^{29}Si/^{28}Si$ (Fig. 2) and initial $^{26}Al/^{27}Al$ ratios (Fig. 1*b*) and the largest ^{46}Ti, ^{49}Ti, and ^{50}Ti excesses (Fig. 3) of the Y grains. It is possible that it has a different origin than the other Y grains. Unfortunately, we could not measure the Ti isotopes in the two grains that have even larger $^{12}C/^{13}C$ and $\Delta^{30}Si/^{28}Si$ ratios, KJGM1-337-3 and KJH5-851 (see Table 1). It remains to be seen whether grains with such C and Si isotopic compositions also have extreme Ti isotopic ratios.

Because the theoretically predicted neutron-capture synthesis of ^{50}Ti depends on the amount of ^{13}C in the intershell, for metallicity $Z = 0.01$ we show in Figure 11 the theoretical predictions for the case u2, an increase of the assumed ^{13}C pocket by a factor of 2, and the case d3, a decrease by a factor of 3, relative to the standard case (Lugaro et al. 1999). While in the d3 case $^{50}Ti/^{48}Ti$ ratios are lower than in the standard case, the reverse is true for the u2 case and predicted ratios almost reach those of the extreme grain KJGM1-158-5.

4.2.3. *Number of Stellar Sources of Y Grains*

Alexander (1993) used various astronomical data and assumptions to estimate that some 10–100 AGB stars contributed SiC dust to the early solar system. Since Y grains make up only ~1% of presolar SiC, it is likely that only a small fraction of these presolar AGB stars were the low-metallicity progenitors of Y grains. We can estimate the minimum number of sources from the isotopic data. Most of the Y grains have Si isotopic compositions lying close to the original Y grain line defined by Hoppe et al (1994), implying a relatively narrow range of initial compositions for the parent stars. In fact, when projected onto the "Galactic" line on a Si 3-isotope plot, a majority of the grains' compositions overlap within the error limits. Taking the errors into account, the projected compositions indicate that only very few (~4–5) unique compositions are required to explain the data. This result holds if the Y grains reported in other studies are included in the analysis as well. Moreover, as discussed above, stars with a range of masses are required to explain the spread of the data in Figure 8. Assuming all Y grains formed in stars of $Z = 0.01$, visual inspection of Figure 8*b* suggests that the bulk of the data can be explained within errors by a small number of model AGB stars, again perhaps four to five. The most extreme grains may well require additional sources but it is clear

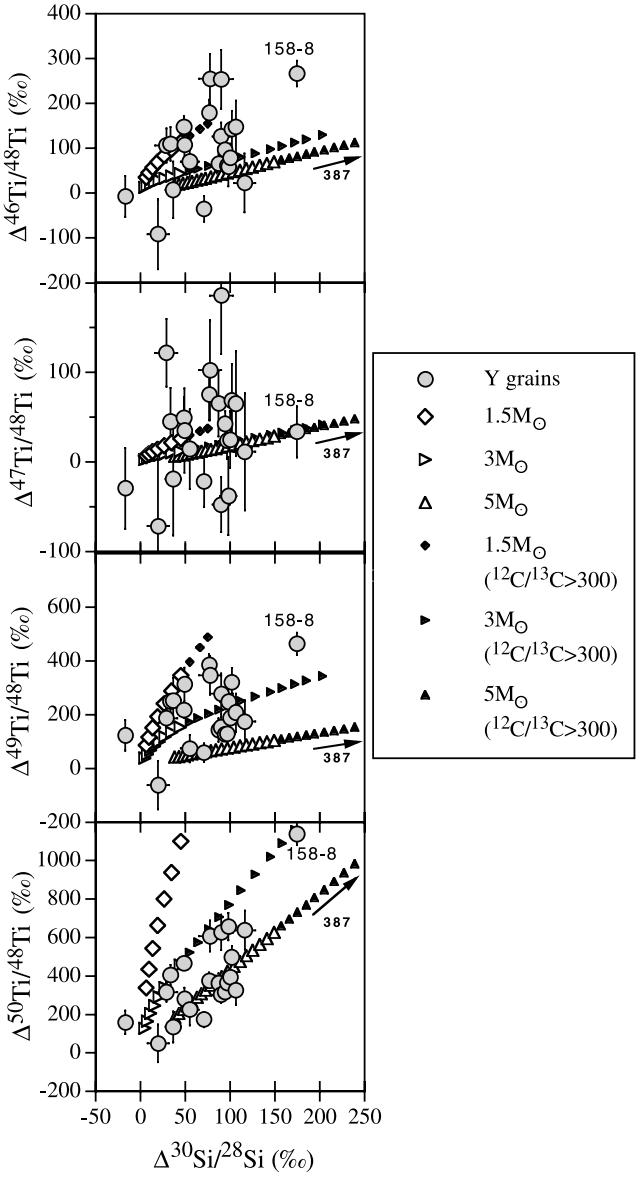

FIG. 10*a*

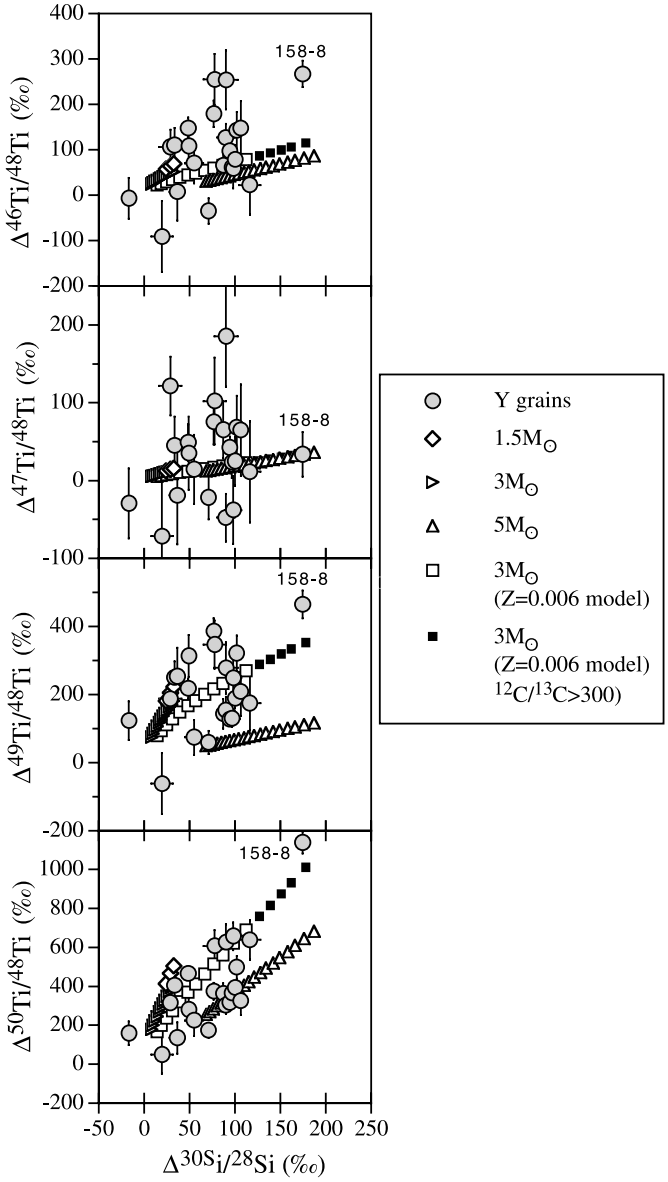

FIG. 10*b*

FIG. 10.—Titanium isotopic ratios of Y grains corrected for the Galactic component are plotted against the corrected $^{30}Si/^{28}Si$ ratios and compared with the results of AGB models for $Z = 0.006$ (*a*) and $Z = 0.01$ (*b*). As in Fig. 8 for $Z = 0.006$, we used simulations for the 1.5 and 5 $M_\odot$ stars, full stellar models for the other cases. The symbols are the same as in Fig. 8. Of the theoretical predictions, the open symbols are for $100 < {}^{12}C/{}^{13}C < 300$, the filled symbols are for $^{12}C/^{13}C > 300$. The arrows in (*a*) indicate that the $\Delta^{30}Si/^{28}Si$ ratios of the 5 $M_\odot$ model extend to a value of 387. See the electronic edition of the Journal for a color version of this figure.

that the Y grain data can be explained by a relatively small number of low-metallicity AGB star parents, probably less than 10.

4.2.4. *Galactic Evolution of the Silicon Isotopes*

One interesting problem following from the isotopic compositions of the Y grains is the following. The models that best account for the grain data are those with metallicity of approximately $Z = 0.01$, that means half the solar metallicity. If we use the Timmes & Clayton (1996) model for the Galactic evolution of the Si isotopes, a metallicity of $Z = 0.01$ (i.e., [Fe/H] ≈ -0.3) corresponds to an isotopic ratio of at most 0.75 times solar for the Si isotopes, or a $\delta^{30}Si/^{28}Si$ value of less than $-250‰$. However, the average AGB-corrected $\delta^{30}Si/^{28}Si$ value of the Y grains is only $-20‰$ (Fig. 7) or $-38.7‰$ if we project the Si isotopic ratios of the Y grains not onto the mainstream correlation line but onto the slope-one line passing through the solar isotopic composition.

In Figure 12 we plot the evolution of the $^{30}Si/^{28}Si$ ratio from Figure 4 of Timmes & Clayton (1996) versus metallicity Z. We also plot the average $^{30}Si/^{28}Si$ ratios and metallicities inferred from the mainstream and Y grains (this paper) and from Z grains (Hoppe et al. 1997; Zinner et al. 2000). The range in inferred Si isotopic ratios and the uncertainties in the metallicity are schematically (there is no way to accurately estimate the uncertainty in the metallicity) expressed in the form of shaded ellipses. As can be seen from the figure, in the Timmes & Clayton model the Si isotopic ratios in the Galactic disk do not increase linearly with metallicity but initially increase more rapidly up to a metallicity of $Z \sim 0.01$, when the evolutionary slope becomes shallower. The reason for this behavior is that contributions from Type Ia SNe, which produce mostly pure ^{28}Si, start to

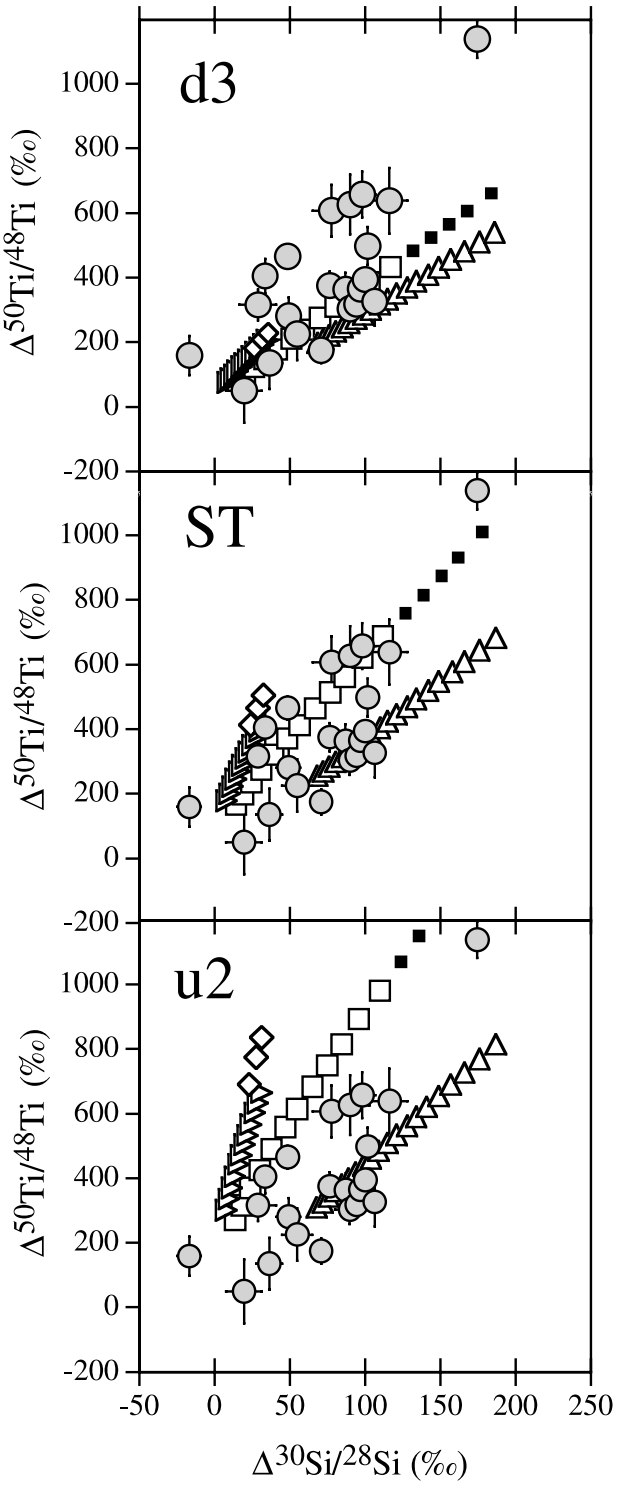

FIG. 11.—$^{50}Ti/^{48}Ti$ ratios of Y grains corrected for the Galactic component are plotted against the corrected $^{30}Si/^{28}Si$ ratios and compared with the results of AGB models for $Z = 0.01$ for three assumed values for the ^{13}C abundance in the region between the AGB H and He shells (intershell). In the d3 case the ^{13}C abundance is one-third and in the u2 case twice the amount assumed for the standard case (ST) (Lugaro et al. 1999). Symbols are the same as in Figs. 8 and 10. See the electronic edition of the Journal for a color version of this figure.

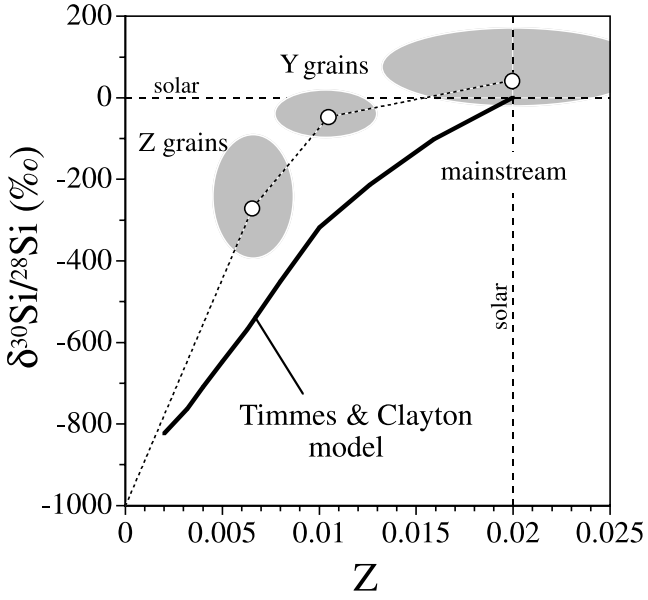

FIG. 12.—Evolution of the $^{30}Si/^{28}Si$ ratio (expressed as δ-values) as function of metallicity Z in the Galactic disk. The results of the Galactic evolution model of Timmes & Clayton (1996), adjusted so that the ratio is solar at solar metallicity, are compared with the Si ratios and metallicities inferred from mainstream and Y grains (this work) as well as SiC grains of type Z (Zinner et al. 2000). The shaded ellipses express the range of $^{30}Si/^{28}Si$ ratios inferred from individual grains and the uncertainty in metallicity for different types of grains.

become important in the later phases of Galactic evolution (Timmes et al. 1995). The inference from the grain data is an even more pronounced change in the evolution of the Si isotopic ratios. Taken at face value, this would mean that at the time preceding solar system formation the Si isotopic ratios in the Galactic disk evolve much more slowly than the Timmes & Clayton (1996) model predicts. Lugaro et al. (1999) have pointed out that the rate of the Timmes & Clayton (1996) evolution at the time of solar system formation depends on the relative proportions of Type II and Type Ia SN contributions to the ISM. If, as Woosley et al. (1997) assumed, the Type Ia contributions were higher than those adopted in the Timmes & Clayton (1996) model, the Si isotopes evolve more slowly toward heavier compositions. The Y grain data clearly point in this direction, however, it remains to be seen whether the required change in the relative contributions from Type Ia and Type II SNe are supported by other observations.

Some caution should be used in drawing broad conclusions about Galactic evolution from the Y grains. Assuming they indeed originated in low-metallicity AGB stars, the results of the previous section indicate that they formed in a small number of such stars, with only a small likelihood that the Y grains are a representative sample. Nontheless, we note in the context of the present discussion that a much slower rate of increase of the Si isotopic ratios than that of the Timmes & Clayton model is supported by the isotopic composition of present-day Galactic cosmic rays, which are believed to sample the local Galactic environment. Satellite measurements indicate that their Si isotopic ratios are solar within approximately 10% (Lukasiak et al. 1994; Duvernois et al. 1996; Connell & Simpson 1997; Webber, Lukasiak, & McDonald 1997), whereas much larger ratios are expected if

the Si isotopes in the solar neighborhood of the Galaxy evolved according to the Timmes & Clayton (1996) model (Fig. 12, see also their Fig. 6).

5. CONCLUSION

Presolar SiC grains of type Y, making up $\sim 1\%$ of SiC grains with sizes greater than 2 μm, seem to have originated in C-rich AGB stars, like the mainstream grains, but from stars with lower metallicity. Three major characteristics of the grains point in this direction: (1) their large $^{12}C/^{13}C$ ratios (by definition Y grains have $^{12}C/^{13}C > 100$), (2) their Si isotopic compositions, which plot to the right of the mainstream correlation line on a Si 3-isotope plot, and (3) their, on average, lower $^{29}Si/^{28}Si$ ratios than those of the mainstream grains. In addition, one grain has extremely large ^{49}Ti and ^{50}Ti excesses. AGB stars of low metallicity are expected to dredge up more ^{12}C and more material that experienced neutron capture than do stars of solar metallicity. The envelopes of such stars are therefore expected to have higher $^{12}C/^{13}C$, $^{30}Si/^{28}Si$, $^{49}Ti/^{48}Ti$, and $^{50}Ti/^{48}Ti$ ratios than mainstream grains, whose Si and Ti isotopic compositions are, in principle, explained by AGB stars of solar metallicity. We have compared the C, Si, and Ti isotopic compositions of Y grains with theoretical predictions of AGB stars with masses of 1.5, 3, and 5 $M_\odot$ and metallicities $Z = 0.006$, 0.01, and 0.02 (solar). Models of stars with solar metallicity cannot account for the grain data. The AGB models of lower metallicity, on the other hand, can explain the measured isotopic compositions reasonably well, the best agreement being for stars of approximately half solar metallicity ($Z = 0.01$). A range of stellar masses (possibly up to 5 $M_\odot$) for the grain progenitors is also indicated by the data. The present study and data on SiC grains of type Z furthermore suggest that the rate of change of the ratios of the secondary Si isotopes (^{29}Si and ^{30}Si) relative to ^{28}Si in the ISM prior to solar system formation was lower then has been generally assumed, implying larger contributions from Type Ia SNe compared to those from Type II SNe. Such a behavior is supported by the Si isotopic ratios of Galactic cosmic rays.

We are grateful to Oscar Straniero, Maurizio Busso, Alessandro Chieffi, and Marco Limongi for their contributions to the FRANEC model and the AGB nucleosynthesis calculations presented in this paper. We thank Dianne Wooden for an insightful review. R. G. acknowledges support by the McDonnell Center for the Space Sciences that made his visit to Washington University possible. This work was supported by NASA grants NAG5-8336 (S. A. and E. Z.) and NAG5-4297 (R. S. L.) and by MURST Progetto Evoluzione Stellare Confin 98 (R. G.). M. L. acknowledges support from an IPRS scholarship.

REFERENCES

Alexander, C. M. O'D. 1993, Geochim. Cosmochim. Acta, 57, 2869
Alexander, C. M. O'D., & Nittler, L. R. 1999, ApJ, 519, 222
Amari, S., Hoppe, P., Zinner, E., & Lewis, R. S. 1992, ApJ, 394, L43
———. 1995, Meteoritics, 30, 679
Amari, S., Lewis, R. S., & Anders, E. 1994, Geochim. Cosmochim. Acta, 58, 459
Amari, S., Nittler, L. R., Zinner, E., & Lewis, R. S. 1997a, Lunar Planet. Sci., 28, 33
———. 1997b, Meteorol. Planet. Sci., 32, A6
———. 1999, Lunar. Planet. Sci., 30, Abstract 1009 (Houston: Lunar Planet. Sci. Inst.), CD-ROM
———. 2000a, Lunar Planet. Sci., 31, Abstract 1421 (Houston: Lunar Planet. Sci. Inst.), CD-ROM
Amari, S., Zinner, E., & Lewis, R. S. 2000b, Meteorit. Planet. Sci., 35, 997
Amari, S., Anders, E., Virag, A., & Zinner, E. 1990, Nature, 345, 238
Anders, E., & Grevesse, N. 1989, Geochim. Cosmochim. Acta, 53, 197
Bazan, G. 1991, Ph.D. thesis, Univ. Illinois, Urbana-Champaign
Bernatowicz, T. J., Amari, S., Zinner, E., & Lewis, R. S. 1991, ApJ, 373, L73
Bernatowicz, T. J., Cowsik, R., Gibbons, P. C., Lodders, K., Fegley, B., Jr., Amari, S., & Lewis, R. S. 1996, ApJ, 472, 760
Bernatowicz, T., Fraundorf, G., Tang, M., Anders, E., Wopenka, B., Zinner, E., & Fraundorf, P. 1987, Nature, 330, 728
Blöcker, T. 1999, in Asymptotic Giant Branch Stars, ed. T. Le Bertre, A. Lèbre & C. Waelkens (Provo: ASP), 21
Boothroyd, A. I., & Sackmann, I.-J. 1999, ApJ, 510, 232
Busso, M., Gallino, R., Lugaro, M., Straniero, O., Smith, V., & Lambert, D. L. 2000, Mem. Soc. Astron. Italiana, in press
Busso, M., Gallino, R., & Wasserburg, G. J. 1999, ARA&A, 37, 239
Charbonnel, C. 1995, ApJ, 453, L41
Charbonnel, C., Brown, J. A., & Wallerstein, G. 1998, A&A, 332, 201
Choi, B.-G., Wasserburg, G. J., & Huss, G. R. 1999, ApJ, 522, L133
Clayton, D. D., Obradovic, M., Guha, S., & Brown, L. E. 1991, Lunar Planet. Sci., 22, 221
Clayton, D. D., & Timmes, F. X. 1997, ApJ, 483, 220
Connell, J. J., & Simpson, J. A. 1997, in 25th Int. Cosmic-Ray Conference (Durban), ed. M. S. Potgieter, B. C. Raubenheimer & D. J. van der Walt, 3, 381
Dearborn, D. S. P. 1992, Phys. Rep., 210, 367
Dominy, J. F., & Wallerstein, G. 1987, ApJ, 317, 810
Duvernois, M. A., Garcia-Munoz, M., Pyle, K. R., Simpson, J. A., & Thayer, M. R. 1996, ApJ, 466, 457
El Eid, M. 1994, A&A, 285, 915
Gallino, R., Arlandini, C., Busso, M., Lugaro, M., Travaglio, C., Straniero, O., Chieffi, A., & Limongi, M. 1998, ApJ, 497, 388
Gallino, R., Busso, M., & Lugaro, M. 1997, in AIP Conf. Proc. 402, Astrophysical Implications of the Laboratory Study of Presolar Materials, ed. T. J. Bernatowicz & E. Zinner (New York: AIP), 115
Gallino, R., Busso, M., Picchio, G., & Raiteri, C. M. 1990, Nature, 348, 298
Gallino, R., Raiteri, C. M., & Busso, M. 1993, ApJ, 410, 400
Gallino, R., Raiteri, C. M., Busso, M., & Matteucci, F. 1994, ApJ, 430, 858
Gao, X., & Nittler, L. R. 1997, Lunar Planet. Sci., 28, 393
Gilroy, K. K. 1989, ApJ, 347, 835
Gilroy, K. K., & Brown, J. A. 1991, ApJ, 371, 578
Gratton, R., & Sneden, C. 1994, A&A, 287, 927
Hoppe, P., Amari, S., Zinner, E., Ireland, T., & Lewis, R. S. 1994, ApJ, 430, 870
Hoppe, P., Annen, P., Strebel, R., Eberhardt, P., Gallino, R., Lugaro, M., Amari, S., & Lewis, R. S. 1997, ApJ, 487, L101
Hoppe, P., Kocher, T. A., Strebel, R., Eberhardt, P., Amari, S., & Lewis, R. S. 1996a, Lunar Planet. Sci., 27, 561
Hoppe, P., & Ott, U. 1997, in AIP Conf. Proc. 402, Astrophysical Implications of the Laboratory Study of Presolar Materials, ed. T. J. Bernatowicz & E. Zinner (New York: AIP), 27
Hoppe, P., Strebel, R., Amari, S., & Lewis, R. S. 1999, Lunar Planet Sci., 30, Abstract 1256 (Houston: Lunar Planet. Sci. Inst.), CD-ROM
Hoppe, P., Strebel, R., Eberhardt, P., Amari, S., & Lewis, R. S. 1996b, Geochim. Cosmochim. Acta, 60, 883
———. 1996c, Science, 272, 1314
Huss, G. R., Hutcheon, I. D., & Wasserburg, G. J. 1997, Geochim. Cosmochim. Acta, 61, 5117
Huss, G. R., & Lewis, R. S. 1995, Geochim. Cosmochim. Acta, 59, 115
Huss, G. R., Fahey, A. J., Gallino, R., & Wasserburg, G. J. 1994, ApJ, 430, L81
Hutcheon, I. D., Huss, G. R., Fahey, A. J., & Wasserburg, G. J. 1994, ApJ, 425, L97
Iben, I., Jr. 1977, in Advanced Stages in Stellar Evolution, ed. P. Bouvier & A. Maeder (Sauverny: Genève Obs.), 1
Iben, I., Jr., & Renzini, A. 1982, ApJ, 263, L23
———. 1984, Phys. Rep., 105, 329
Lambert, D. L. 1981, in Physical Processes in Red Giants, ed. I. Iben, Jr., & A. Renzini (Dortrecht: Reidel), 115
Lambert, D. L., Gustafsson, B., Eriksson, K., & Hinkle, K. H. 1986, ApJS, 62, 373
Larimer, J. W. 1968, Geochim. Cosmochim. Acta, 32, 965
Lattanzio, J., & Forestini, M. 1999, in Asymptotic Giant Branch Stars, ed. T. Le Bertre, A. Lèbre & C. Waelkens (Provo: ASP), 31
Lattanzio, J., Frost, C., Cannon, R., & Wood, P. 1996, Mem. Soc. Astron. Italiana, 67, 729
Lattanzio, J. C., & Boothroyd, A. I. 1997, in AIP Conf. Proc. 402, Astrophysical Implications of the Laboratory Study of Presolar Materials, ed. T. J. Bernatowicz & E. Zinner (New York: AIP), 85
Lewis, R. S., Amari, S., & Anders, E. 1990, Nature, 348, 293
———. 1994, Geochim. Cosmochim. Acta, 58, 471
Lewis, R. S., Tang, M., Wacker, J. F., Anders, E., & Steel, E. 1987, Nature, 326, 160
Lodders, K., & Fegley, B., Jr. 1995, Meteoritics, 30, 661

Lodders, K., & Fegley, B., Jr. 1997, in AIP Conf. Proc. 402, Astrophysical Implications of the Laboratory Study of Presolar Materials, ed. T. J. Bernatowicz & E. Zinner (New York: AIP), 391
———. 1998, Meteorit. Planet. Sci., 33, 871
Lugaro, M., Zinner, E., Gallino, R., & Amari, S. 1999, ApJ, 527, 369
Lukasiak, A., Ferrando, P., McDonald, F. B., & Webber, W. R. 1994, ApJ, 426, 366
Nittler, L. R. 1996, Ph.D. thesis, Washington Univ.
Nittler, L. R., Alexander, C. M. O'D., Gao, X., Walker, R. M., & Zinner, E. 1997, ApJ, 483, 475
———. 1994, Nature, 370, 443
Nittler, L. R., Amari, S., Zinner, E., Woosley, S. E., & Lewis, R. S. 1996, ApJ, 462, L31
Nittler, L. R., et al. 1995, ApJ, 453, L25
Ott, U., & Begemann, F. 1990a, Lunar Planet. Sci., 21, 920
———. 1990b, ApJ, 353, L57
Prombo, C. A., Podosek, F. A., Amari, S., & Lewis, R. S. 1992, Lunar Planet. Sci., 23, 1111
———. 1993, ApJ, 410, 393
Richter, S., Ott, U., & Begemann, F. 1993, in Nuclei in the Cosmos, ed. F. Käppeler & K. Wisshak (Bristol: Inst. Phys.), 127
Sharp, C. M., & Wasserburg, G. J. 1995, Geochim. Cosmochim. Acta, 59, 1633
Smith, V. V., & Lambert, D. L. 1990, ApJS, 72, 387
Sneden, C., Pilachowski, C. A., & Vandenberg, D. A. 1986, ApJ, 311, 826
Stone, J., Hutcheon, I. D., Epstein, S., & Wasserburg, G. J. 1991, Earth Planet. Sci. Lett., 107, 570
Straniero, O., Chieffi, A., Limongi, M., Busso, M., Gallino, R., & Arlandini, C. 1997, ApJ, 478, 332
Straniero, O., Chieffi, A., Limongi, M., Gallino, R., & Busso, M. 2000, Mem. Soc. Astron. Italiana, in press
Tang, M., & Anders, E. 1988, Geochim. Cosmochim. Acta, 52, 1235
Timmes, F. X., & Clayton, D. D. 1996, ApJ, 472, 723
Timmes, F. X., Woosley, S. E., & Weaver, T. A. 1995, ApJS, 98, 617
Travaglio, C., Gallino, R., Amari, S., Zinner, E., Woosley, S., & Lewis, R. S. 1999, ApJ, 510, 325
Virag, A., Wopenka, B., Amari, S., Zinner, E., Anders, E., & Lewis, R. S. 1992, Geochim. Cosmochim. Acta, 56, 1715
Wallerstein, G., & Morell, O. 1994, A&A, 281, L37
Wasserburg, G. J., Boothroyd, A. I., & Sackmann, I.-J. 1995, ApJ, 447, L37
Webber, W. R., Lukasiak, A., & McDonald, F. B. 1997, ApJ, 476, 766
Wheeler, J. C., Sneden, C., & Truran, J. W. 1989, ARA&A, 27, 279
Wood, P. R. 1981, in Physical Processes in Red Giants, ed. I. Iben, Jr., & A. Renzini (Dordrecht: Reidel), 135
Woosley, S. E., Hoffman, R. D., Timmes, F. X., Weaver, T. A., & Thielemann, F.-K. 1997, Nucl. Phys. A, 621, 445c
Woosley, S. E., & Weaver, T. A. 1995, ApJS, 101, 181
Zinner, E. 1998, Annu. Rev. Earth Planet. Sci., 26, 147
Zinner, E., Amari, S., Gallino, R., & Lugaro, M. 2000, Nuclei in the Cosmos 2000 (Denmark: Aarhus)
Zinner, E., Amari, S., & Lewis, R. S. 1991, ApJ, 382, L47
Zinner, E., Tang, M., & Anders, E. 1989, Geochim. Cosmochim. Acta, 53, 3273